

Design of a Two-Dimensional Supersonic Nozzle for use in Wind Tunnels

a project presented to
The Faculty of the Department of Aerospace Engineering
San José State University

in partial fulfillment of the requirements for the degree
Master of Science in Aerospace Engineering

by

Yousheng Deng

May 2018

approved by

Dr. Fabrizio Vergine
Faculty Advisor



San José State
UNIVERSITY

© 2018

Yousheng Deng

ALL RIGHTS RESERVED

The Designated Project Advisor(s) Approves the Thesis Titled

DESIGN OF A TWO-DIMENSIONAL SUPERSONIC NOZZLE FOR USE IN WIND
TUNNELS

by

Yousheng Deng

APPROVED FOR THE DEPARTMENT OF AEROSPACE ENGINEERING
SAN JOSÉ STATE UNIVERSITY

May 2018

Dr. Fabrizio Vergine Department of Aerospace Engineering Advisor

ABSTRACT

DESIGN OF A TWO-DIMENSIONAL SUPERSONIC NOZZLE FOR USE IN WIND TUNNELS

By Yousheng Deng

This paper outlines the theory, process, and verification of the design of a two-dimensional nozzle. Fundamental concepts of isentropic and non-isentropic flows are reviewed. Then a gradual-expansion nozzle is designed using the two-dimensional method of characteristics, modified to include a gradual expansion section. Inviscid CFD simulations are then ran to verify the final nozzle is capable of accelerating the flow to the wanted supersonic speed without any shocks. Viscous simulations are then ran to account for boundary layer effects on the walls.

ACKNOWLEDGEMENTS

I would like to sincerely thank my parents for their endless support and encouragement over the course of this project. I would also like to thank my advisor, Dr. Fabrizio Vergine, for his knowledge and guidance throughout this project.

Table of Contents

List of Symbols	iv
List of Figures	v
List of Tables	vi
1 Introduction	1
1.1 Motivation	1
1.2 Literature Review	2
1.2.1 Wind Tunnel Components	2
1.2.2 de Laval Nozzle	2
1.3 Flow Through a CD Nozzle	4
1.4 Project Proposal	5
1.5 Methodology	5
2 Reduced Order Model.....	6
2.1 Isentropic Flow.....	6
2.2 Flow With Shocks	8
2.2.1 Normal Shock	9
2.2.2 Oblique Shock.....	10
3 Finalization of the Nozzle.....	12
4 Nozzle Contour Design	17
4.1 Method of Characteristics: Derivation	17
4.2 Method of Characteristics: Application	19
5 CFD Analysis and Verification	24
5.1 Mesh Generation and Problem Setup.....	24
5.2 Results and Discussion.....	28
5.2.1 Inviscid Simulation Results	28
5.2.2 Viscous Simulation Results	30
6 Conclusion	33
7 Future Works	34
References.....	35
Appendix A: Reduced Order Model MATLAB Code.....	36
Appendix B: Trade Study MATLAB Code	42
Appendix C: Method of Characteristics	45

Appendix D: Nozzle Contour Coordinates	49
Appendix E: SST Variable Definitions and Constants	57

List of Symbols

Symbol	Definition	Units (English)
A	Area	in ²
A*	Throat Area	in ²
k	Turbulent Kinetic Energy	ft ² /s ²
M	Mach Number	-----
P	Pressure	psi
Pr	Prandtl Number	-----
T	Temperature	Rankine
t	Time	s
u	Velocity along x-axis	ft/s
V	Volume	in ³
v	Velocity along y-axis	ft/s
Greek Symbols		
β	Shock Angle	deg or rad
γ	Specific Heat	-----
μ	Local Mach Angle	deg or rad
ν	Prandtl-Meyer Function	deg or rad
θ	Mach Angle	deg or rad
ω	Dissipation Rate	1/s
Subscripts		
() ₀	Total	-----
Acronyms		
CFD	Computational Fluid Dynamics	-----
CAD	Computer Aided Design	-----
CD	Convergent-Divergent	-----

List of Figures

Figure 2.1	The geometry of the nozzle. The throat location is denoted by a red line	7
Figure 2.2	Pressure ratio and Mach number of isentropic nozzle flow at Mach 5. Mach 1 and 8	
Figure 2.3	Pressure ratio and Mach number of isentropic supersonic flow and supersonic flow with a normal shock. Mach 1 and the throat location are denoted by red lines. The shock location is denoted by a green line.....	9
Figure 3.1	Schematic of the wind tunnel with the control volume in red	12
Figure 3.2	Runtime vs Mach for overexpanded flow at various exit areas.....	14
Figure 3.3	Runtimes vs plenum pressure for Mach 3 flow at various exit areas	15
Figure 3.4	Length of shock-free area vs plenum pressure for Mach 3 at various exit areas....	16
Figure 3.5	Length of shock-free area vs runtimes for Mach 3 at various exit areas	16
Figure 4.1	Preliminary Method of Characteristics with Wall Points	20
Figure 4.2	Preliminary Method of Characteristics with Labeled Points	20
Figure 4.3	10-Line Method of Characteristics with Internal Lines.....	23
Figure 4.4	Method of Characteristics Nozzle Contour	23
Figure 5.1	SolidWorks Drawing	25
Figure 5.2	CFD-GEOM Boundary Labels	25
Figure 5.3	CFD-GEOM Mesh	25
Figure 5.4	CFD-FASTRAN Model	26
Figure 5.5	Pressure Contour of Converged Inviscid Simulation	28
Figure 5.6	U Velocity Contour of Converged Inviscid Simulation	29
Figure 5.7	V Velocity Contour of Converged Inviscid Simulation	29
Figure 5.8	Mach Contour of Converged Inviscid Simulation.....	29
Figure 5.9	Pressure Contour of Converged Viscous Simulation	30
Figure 5.10	U Velocity Contour of Converged Viscous Simulation	30
Figure 5.11	V Velocity Contour of Converged Viscous Simulation	31
Figure 5.12	Mach Contour of Converged Viscous Simulation.....	31

List of Tables

Table 3.1	Final Nozzle Parameters	15
Table 4.1	10-Line Method of Characteristics. The wall points are highlighted in yellow.....	21
Table 5.1	Inviscid Inlet Boundary Conditions	26
Table 5.2	Inviscid Volume Initial Conditions.....	26
Table 5.3	Turbulent Model Options.....	27
Table 5.4	Turbulent Inlet Boundary Conditions	27

1 Introduction

1.1 Motivation

On October 14, 1947, the sound barrier was broken for the first time. Capt. Charles E. “Chuck” Yeager piloted the rocket-powered Bell X-1 to a speed of Mach 1.07 and from that day forward, the world of supersonic flight was finally reached. Since then, large amounts of funding have been allocated to bring supersonic flight closer and more accessible to people. From planes like the Douglas D-558-2 Skyrocket, the first aircraft to exceed Mach 2, to the Aérospatiale/BAC Concorde, the first commercial plane to achieve sustained supersonic flight, our understanding of supersonic fluid flow has improved drastically.

In recent years, there has even been a resurgence of the idea of supersonic transportation, with companies like Boom Technology and Aerion Corporation working hard to design supersonic business jets [1-4]. There are multiple ways of testing their models, such as computational fluid dynamics (CFD) analysis or supersonic wind tunnel tests. Of the two, wind tunnels are more realistic and therefore give better data.

Wind tunnels have been in use for more than a century. From the early works of Benjamin Robins to the one used by the Wright brothers, wind tunnels have given researchers a way to bring the chaotic currents from the skies above to ground stations where the airflow can be studied and experimented on in a controlled environment. A well-designed tunnel can provide accurate data, saving researchers much time, effort, and other resources.

1.2 Literature Review

1.2.1 Wind Tunnel Components

Supersonic wind tunnels are comprised of multiple parts. The four major sections, listed from beginning to end, are the inlet, nozzle, test section, and diffuser. The inlet is where the air first enters the core. Some tunnels use a fan to draw in outside air, while others use pressurized tanks to force in air. Regardless of the method of intake, the aerodynamic properties of the incoming stream are rarely the ones that researchers want. The incoming air is therefore stabilized and blown through a nozzle to enter the test section at the desired conditions. In order to accelerate a flow to a specific desired Mach number without any shocks forming, the pressure upstream of the nozzle must be a certain order of magnitude above the pressure at the end of the tunnel. This is achieved with a diffuser.

While the air flows through the test section containing the experimental model and data is being collected, it passes through a diffuser designed to lower the speed, pressure, and reduce total pressure losses. The lower the losses, the lower the pressure in front of the nozzle needs to be to prevent shocks in the divergent nozzle. The nozzle also brings the flow to ambient conditions before either circling back to the start or being expelled outside. This report will focus specifically on the nozzle section for a supersonic wind tunnel.

1.2.2 de Laval Nozzle

A de Laval nozzle, also known as a converging diverging (CD) nozzle, is a tube that is pinched in the middle, similar in shape to an hourglass. As its name suggests, a CD nozzle has two parts: the converging section upstream of the pinched throat and a diverging section downstream of the pinched throat. A convergent nozzle is one in which the cross-sectional area

decreases as the flow moves downstream. The free stream flow enters a convergent section at subsonic speeds ($M < 1$) and speeds up due to the decreased area to maintain a constant mass flow rate. A properly designed convergent section will accelerate the flow to reach sonic ($M = 1$) at the throat where the cross-sectional area is the smallest. It will then enter the divergent section, in which the cross-sectional area increases as the flow moves downstream. Unlike subsonic flow, sonic and supersonic flows speed up as the area increases.

There are two types of supersonic divergent nozzles: gradual expansion and minimum length [6,9]. Gradual expansion nozzles start with a cross-sectional area of the throat and gradually expand outwards. In this section, the contours of the walls bend away from the free stream, allowing the sonic flow more area to expand and accelerate. It then bends towards the flow, straightening it as it enters the test section. The point on the wall at which the contour changes from bending away from the free stream to bending towards the free stream, is known as the point of inflection.

Minimum length nozzles also have an expansion and straightening section, but the axial length of the expansion section is much smaller than that of the straightening section. This type of nozzle achieves supersonic flow with the shortest length, saving weight but reducing flow quality.

Minimum length nozzles are used primarily on rockets where rapid expansion and minimal weight are a necessity. These applications do not care about the quality of the exit flow. Gradual expansion nozzles, on the other hand, are longer and heavier but achieve much better exit flow quality. This trait is of great importance in applications such as wind tunnels where accurate flow conditions are crucial to ensure the test model receives uniform airflow.

1.3 Flow Through a CD Nozzle

In an isentropic system with quasi-one-dimensional flow [15], for a given flow upstream of the convergent section, only one ratio between the nozzle inlet cross-sectional area and the throat cross-sectional area (inlet area ratio) will cause the flow to accelerate to sonic at the throat. The ratio between the nozzle outlet pressure and the inlet pressure must also be below a certain value. This pressure ratio value is unique to each free stream Mach number. As long as both conditions are met, the flow at the throat will be sonic. Further decreasing the outlet pressure will not cause the speed of the flow at the throat to increase because the flow chokes. However, depending on how much the pressure is decreased, it may cause a normal shock to form in the divergent section.

Accelerating a sonic flow in a divergent nozzle to a given Mach number is also tied to a single area ratio and pressure ratio. In this case, since the throat pressure is already defined by the convergent section, the exit pressure is set at a particular value. This particular value is the pressure of the flow when it reaches the end of the CD nozzle. However, the exit pressure and the back pressure might not be equal to each other. This pressure discontinuity is corrected by the flow through oblique shock waves and expansion waves. If the exit pressure is below the back pressure, the nozzle is said to be overexpanded. In this situation, a series of oblique shock waves form at the exit of divergent nozzle to compress the flow. On the other hand, if the exit pressure is below the back pressure, the nozzle is underexpanded and expansion waves form at the exit to further expand the flow. Neither is desirable. The best case, and the design goal of the nozzle, is for the exit pressure to equal the back pressure.

1.4 Project Proposal

The goal of this project is to study and design a two-dimensional (2-D) supersonic nozzle for use in the wind tunnel of the university. Special focus will be placed on understanding the flow characteristics and wall contour geometry, taking care to reduce viscous effects and prevent any shocks from forming.

1.5 Methodology

A thorough understanding of the theory behind such a problem must first be established. In the beginning, various topics of supersonic flow and nozzle design will be explored. These include topics such as compressible flow, shock and expansion wave theory, two-dimensional method of characteristics, and viscous effects. Once a satisfactory understanding of the underlying theory has been obtained, publications for a state-of-the-art design of 2-D nozzles will be checked and studied.

Computer aided design (CAD) and computational fluid dynamics (CFD) analysis will be used to provide validation results to lower order modeling provided by the method of characteristics. SolidWorks will be used to draw and constrain the geometry and contours of the nozzle. The geometry will then be imported into ESI CFD-GEOM where the drawing will be meshed and boundary conditions will be set.

After simulations, the results will be analyzed and if necessary, the design will be iterated until it is determined that the nozzle has successfully accelerated a flow to the desired supersonic speeds with acceptable flow quality.

2 Reduced Order Model

During the preliminary design, it is necessary to come up with a reduced order model of the problem. Not only does this help to predict the actual running conditions, it also serves as a form of visual aid and verification. A MATLAB program has been written to accomplish this. This program takes in the geometry of the nozzle walls along with gas properties, and plots the pressure ratio, Mach number, and, if it exists, a normal shock. As the final design tunnel can be used either in a closed configuration as part of a wind tunnel or as a free jet, it is necessary to test out its limits.

2.1 Isentropic Flow

For this preliminary design, the core flow will be assumed to be isentropic, or both adiabatic and inviscid. This means that no heat has been added. Isentropic flow in a wind tunnel is the ideal type of flow and is the design goal of the supersonic nozzle.

There are several assumptions made to assume isentropic flow. First, the viscosity in the core flow is very low. Thus, it has a very high Reynolds number. On the other hand, viscous effects near the walls will be much higher, resulting in a much lower Reynolds number. Since any models placed in the testing chamber will experience mostly core flow, the high viscous effects near the walls can be neglected, thereby allowing the assumption of inviscid flow in the core of the flow. In addition, due to the high speed of the flow, there is barely any time for heat transfer to occur.

A first order approximation of a symmetric CD nozzle was chosen as two straight lines meeting at the throat, shown below in figure 2.1. Using the slope of the lines, the radius and area values at each axial location were determined.

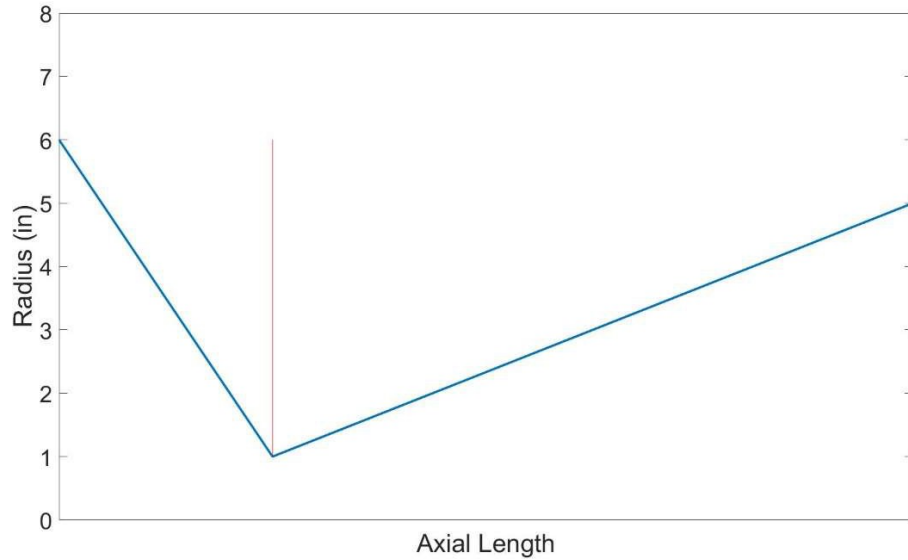


Figure 2.1 The geometry of the nozzle. The throat location is denoted by a red line.

The area-Mach equation shown below was then used to calculate the Mach number at each location, assuming that the flow chokes at the throat. γ is 1.4 for air.

$$\frac{A}{A^*} = \frac{1}{M} \frac{2}{\gamma + 1} \frac{\gamma - 1}{1 + \frac{\gamma - 1}{2} M} \quad (2.1)$$

For a given area ratio, two different values for Mach can satisfy the equation: a subsonic value and a supersonic value. Up to the throat, the flow is subsonic in the convergent section and sonic at the throat. Past the throat, the Mach number can either accelerate to supersonic or decelerate back to subsonic depending on the pressure ratio of the back pressure p and the reservoir stagnation pressure p_0 . This ratio, calculated at each location, is a function of Mach.

$$\frac{p}{p_0} = 1 + \frac{\gamma - 1}{2} M \quad (2.2)$$

Figure 2.2 below shows the changes in pressure ratio and Mach number of a choked isentropic flow at subsonic and supersonic conditions for a generic Mach 5 nozzle.

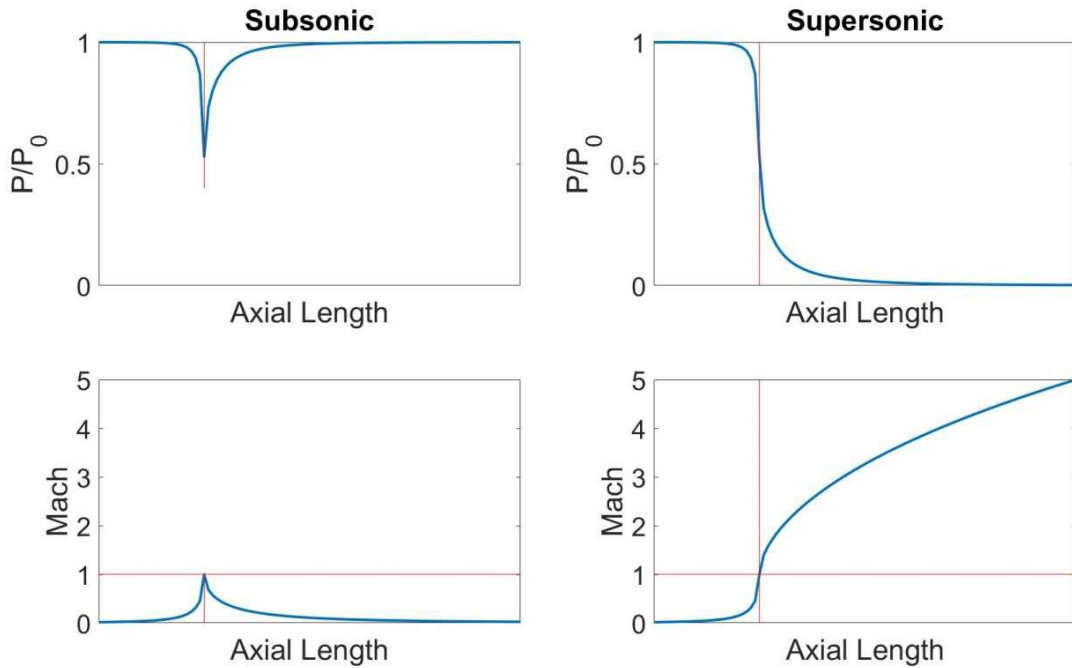


Figure 2.2 Pressure ratio and Mach number of isentropic nozzle flow at Mach 5. Mach 1 and the throat location are denoted by red lines.

From the inlet to the throat, the pressure ratios and Mach numbers for both subsonic and supersonic flow are identical. At the throat, the pressure ratio is 0.528 and the Mach number is one. Downstream of the throat, if the pressure ratio increases, then the flow becomes subsonic. If the pressure ratio decreases, then the flow becomes supersonic. This goes to show that for a choked isentropic flow, whether the flow is subsonic or supersonic depends on if the initial pressure ratio is greater than or less than 0.528.

2.2 Flow With Shocks

Non-isentropic flows have a sharp increase in entropy somewhere along the flow. Most commonly, this is caused by shockwaves forming in the nozzle. A shock wave is an extremely thin region, typically on the order of 10^{-5} cm, across which the flow properties can change

drastically [15]. It can be either an oblique shock, which is situated at an angle, or a normal shock, which is normal to the flow. In both cases, the pressure increase is almost discontinuous.

2.2.1 Normal Shock

Having a normal shock form in the convergent nozzle is detrimental to maintaining a proper flow quality. The total pressure sharply drops and the Mach number always becomes subsonic as shown in the equation below.

$$M = \frac{1 + [(\gamma - 1)/2]M}{\gamma M - (\gamma - 1)/2} \quad (2.3)$$

Following the shock, a subsonic flow in a divergent nozzle will always slow down. This is accompanied by the aforementioned drop in total pressure, resulting in a higher pressure ratio. Afterwards, the flow remains isentropic until it reaches the exit of the nozzle, show below in figure 2.3.

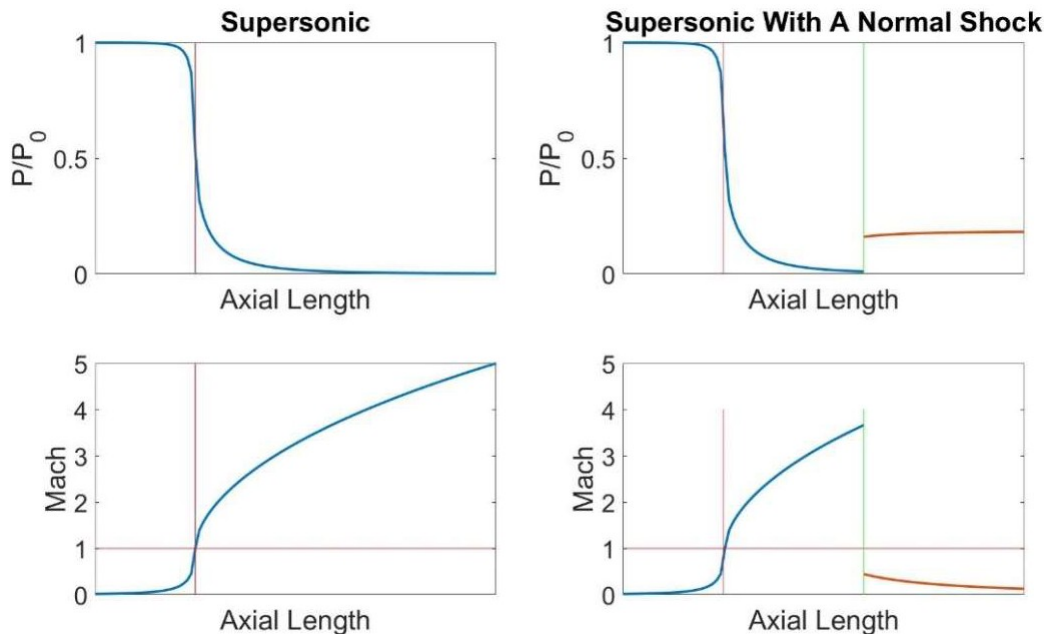


Figure 2.3 Pressure ratio and Mach number of isentropic supersonic flow and supersonic flow with a normal shock. Mach 1 and the throat location are denoted by red lines. The shock location is denoted by a green line.

The location of the normal shock is determined such that after the shock, the isentropic flow arrives at the exit with the same pressure as the ambient air. In the MATLAB model, the normal shock is assumed to be at each axial location downstream of the throat. The multiple instances of the flow then follow isentropic conditions to the exit of the nozzle. The multiple exit pressures are compared with an initially stated value of the ambient pressure and whichever instance achieves the exit pressure closest to the initial value, that instance is assumed to have the most accurate location of the normal shock.

As the total pressure increases, the location of the normal shock will move down the length of the divergent nozzle. At a certain pressure ratio, the normal shock will be at the exit of the nozzle. This is a special case of an overexpanded flow. The pressure ratio across a normal shock is calculated using the following equation.

$$\frac{p}{p_0} = 1 + \frac{2\gamma}{\gamma + 1} M^2 - 1 \quad (2.4)$$

Combining equations 2.2 and 2.4, a third pressure ratio $\frac{p_{11}}{p_0}$ is formed. The flow in a nozzle first becomes sonic at the throat at a pressure ratio of 1.893. Between that and $\frac{p_{11}}{p_0}$, a normal shock forms. At $\frac{p_{11}}{p_0}$, the normal shock is at the exit.

2.2.2 Oblique Shock

If the pressure ratio increases beyond $\frac{p_{11}}{p_0}$, but does not get high enough to achieve isentropic flow, oblique shocks form at the exit. These shockwaves are formed at an angle β to the flow. Similar to a normal shock, an oblique shock forms when the exit pressure of the nozzle is lower than the ambient pressure of the surrounding space. The pressure increase across an oblique shock serves to equalize the exit pressure with the ambient pressure, though the pressure

increase is not nearly as drastic as the increase across a normal shock. Accompanying the pressure increase is a Mach decrease. The resulting flow is slower, though it may remain supersonic.

Oblique shocks are governed by the $\theta - \beta - M$ relation in the equation below. This equation relates the upstream Mach number, the oblique shock angle β , and the downstream Mach angle θ .

$$\tan \theta = 2 \cot \beta \frac{M \sin \beta - 1}{M (\gamma + \cot 2\beta) + 2} \quad (2.5)$$

When overexpanded flow occurs in a nozzle, the flow exit conditions are still maintained until it reaches the oblique shockwaves. When situations occur such that fully isentropic flow in the wind tunnel is not possible, overexpanded flow still provides a region of the desired flow conditions, though with the disadvantage of a limited space.

3 Finalization of the Nozzle

The nozzle will be run as a free jet, at least initially. As such, the plenum pressure will have to be high enough to push any normal shocks out of the exit. However, due to structural and material limitations, the air storage tanks cannot withstand a pressure of over 300 psi, so the largest pressure ratio is 20.4. That is enough to operate a Mach 2.6 nozzle at isentropic conditions but the desired Mach number is higher. A fully isentropic flow at high Mach numbers is not possible in a free-jet facility, and the nozzle will have to be designed to run overexpanded to decrease the plenum pressure requirement. The highest possible Mach number capable of being run overexpanded is Mach 5, which requires a total-to-back pressure ratio of 19.7 and an area ratio of 27.07. However, such a high Mach number requires an equally high plenum pressure of 268.2 psi. At choked flow conditions, the wind tunnel can run for 0.19 second before it unstarts. This needs to be lengthened to around 5 seconds in order to allow enough time for observations.

The run time may be estimated using a control volume analysis shown in figure 3.1.

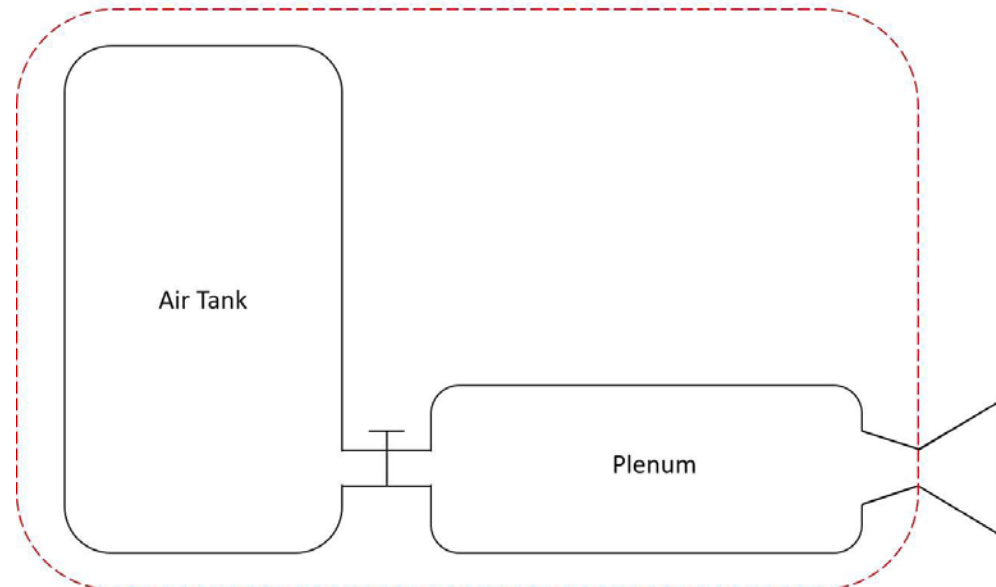


Figure 3.1 Schematic of the wind tunnel with the control volume in red

The control volume analysis equation is shown in equation 3.1 with the integrated form shown in equation 3.2. Substituting terms that involve the Mach number and solving for t results in equation 3.3.

$$\frac{\delta}{\delta t} \rho dV + \rho(V * n)dS = 0 \quad (3.1)$$

$$P(t) \cong -\frac{\dot{m}_{77}}{V} * R * T * t + P(0) \quad (3.2)$$

$$t = \frac{\left(p - \frac{1 + \frac{\gamma-1}{2}M}{1 + \frac{2\gamma}{\gamma+1}(M-1)} * p_n \right) * v * n T_i}{0.532 * \frac{A}{\frac{1}{M} \frac{1}{\gamma+1} \frac{2}{\gamma-1} M^2} * \frac{1 + \frac{\gamma-1}{2}M}{1 + \frac{2\gamma}{\gamma+1}(M-1)} * p_n * R * T_i} \quad (3.3)$$

By plotting the exit Mach number against the run time for various exit areas, interestingly, from figure 3.2 below, it can be seen that supersonic nozzles operated overexpanded in a range from Mach 2 to 4 actually yield the longest run time. This interesting design observation is due to the nonlinear relationship between runtime and Mach number. As the Mach number increases, the throat area decreases, leading to a decrease in the flow rate. The runtime should continuously increase as the Mach number increases. However, as the Mach number increases, the required plenum pressure to push out the normal shock also increases. As the plenum pressure approaches the air tank pressure, the amount of stored air decreases, thus shortening the runtime. The conditions necessary to maintain a Mach 3 flow strike a balance between a shrinking throat area and an increasing plenum pressure.

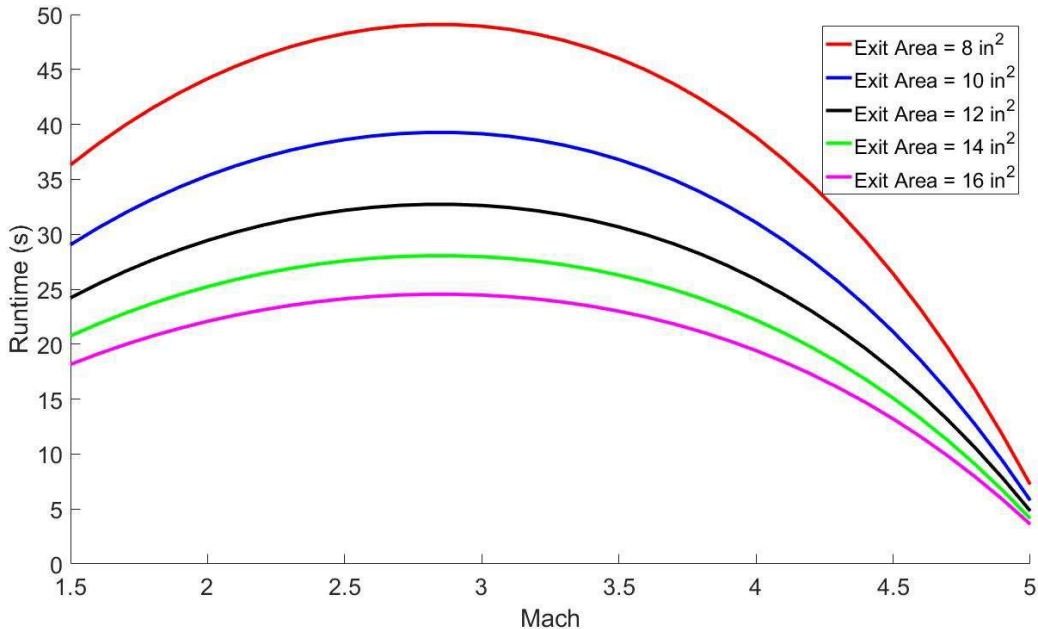


Figure 3.2 Runtime vs Mach for overexpanded flow at various exit areas

Between the five different exit areas shown in figure 3.2, another balance must be struck between runtime and the length of the shock-free area downstream of the exit area of the overexpanded nozzle. As the oblique shocks are generated at the exit, the shock angle and the exit height can be used to determine the length of the shock-free zone. The larger the area, the greater amount of space is available to insert a model. As the exit area increases, the length of the shock-free area increases but the runtime decreases.

Figures 3.3 and 3.4 below show that for a given plenum pressure, an increase in the exit area results in an increase in the length of the shock-free area and a decrease in the runtime. However, figure 3.4 shows that for a desired length of the shock-free area or runtime, a larger exit area maximizes the other value. Increasing the exit area maximizes the length of the shock-free area and runtime and, from figure 3, only marginally affects the run time for a given exit

Mach number. Thus, the exit area will be finalized to be 16 square inches. This and other parameters are shown below in table 3.1.

Finally, it has been decided to set the throat and exit to be equal in width. This serves to limit the flow to only two dimensions, axial and vertical. Preventing the flow from expanding horizontally by having the throat and exit be the same width helps to maintain 2-D flow throughout the nozzle.

Table 3.1 Final Nozzle Parameters

Mach	3
Area ratio	4.23
Throat dimensions (in)	4 X 0.95
Throat area (in ²)	3.78
Exit dimensions (in)	4 X 4
Exit area (in ²)	16
Tank Pressure (psi)	300
Plenum Pressure (psi)	52.26
Run Time (s)	24.47

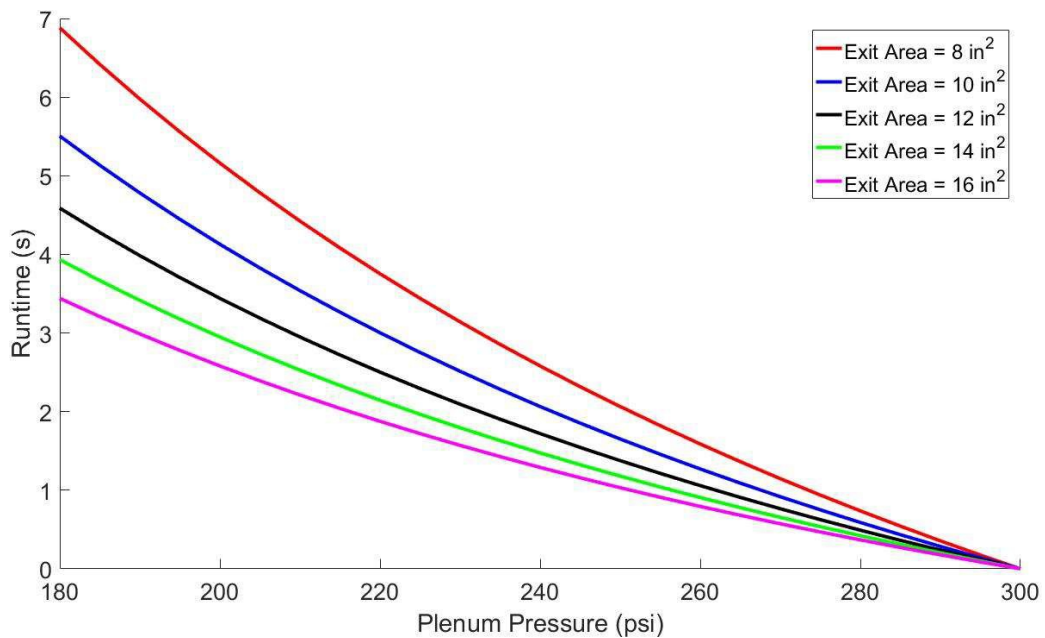


Figure 3.3 Runtimes vs plenum pressure for Mach 3 flow at various exit areas

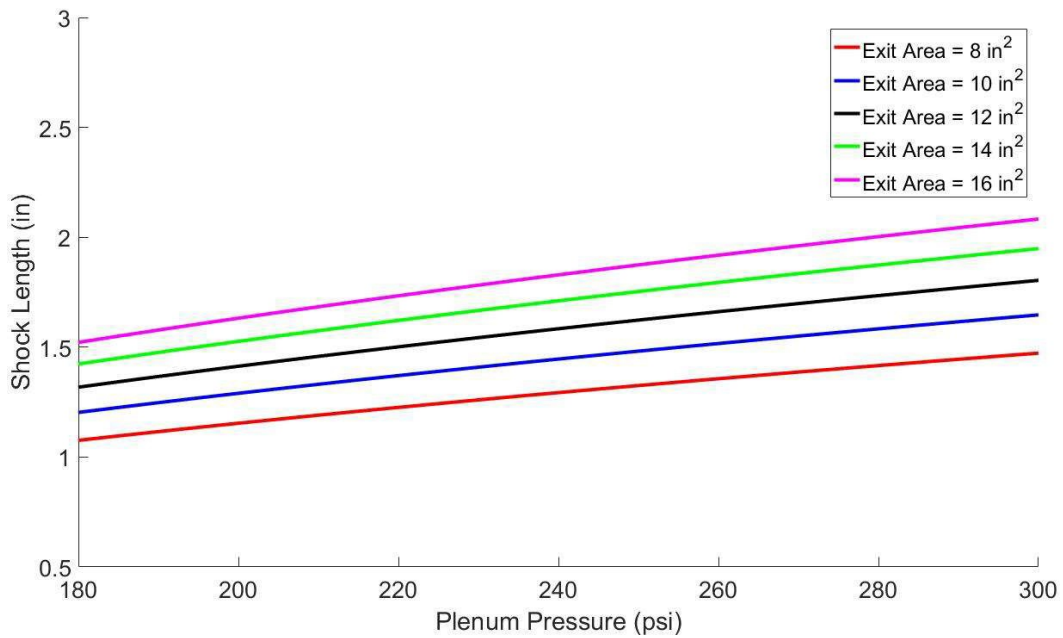


Figure 3.4 Length of shock-free area vs plenum pressure for Mach 3 at various exit areas

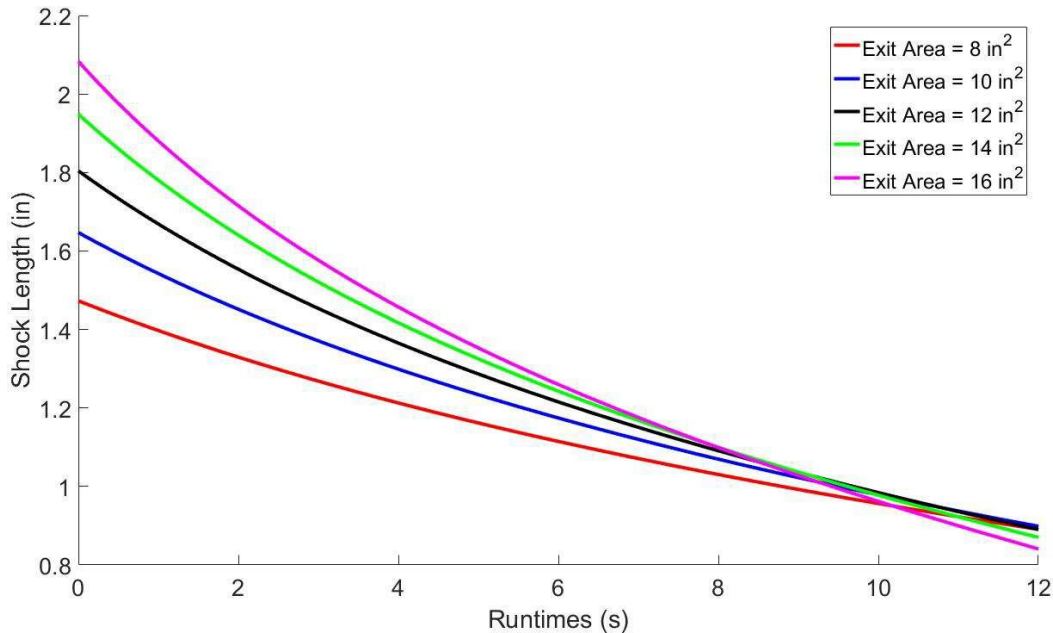


Figure 3.5 Length of shock-free area vs runtimes for Mach 3 at various exit areas

4 Nozzle Contour Design

4.1 Method of Characteristics: Derivation

There exists a definite method for designing a two-dimensional minimum length nozzle, called the method of characteristics. It involves shaping the nozzle contour by finding and solving for a series of characteristic lines. It is derived from the governing equation for a supersonic, steady, inviscid, two-dimensional, irrotational flow shown below.

$$11 - \frac{1}{a} \frac{\delta\phi}{\delta x} - 7 \frac{\delta\phi}{\delta x} + 11 - \frac{1}{a} \frac{\delta\phi}{\delta y} - 7 \frac{\delta\phi}{\delta y} - \frac{2}{a} \frac{\delta\phi}{\delta x} \frac{\delta\phi}{\delta y} = 0 \quad (4.1)$$

Rewriting in terms of the velocity potential and then differentiating results in.

$$11 - \frac{u}{a} \frac{\delta\phi}{\delta x} + 11 - \frac{v}{a} \frac{\delta\phi}{\delta y} - \frac{2uv}{a} \frac{\delta\phi}{\delta x \delta y} = 0 \quad (4.2)$$

$$du = \frac{\delta\phi}{\delta x} dx + \frac{\delta\phi}{\delta x \delta y} dy \quad (4.3)$$

$$dv = \frac{\delta\phi}{\delta y} dx + \frac{\delta\phi}{\delta y} dy \quad (4.4)$$

Equations 4.2, 4.3, and 4.4 can be considered as a system of equations. Solving for 17 using Cramer's rule results in equation 4.5.

$$\frac{\delta\phi}{\delta x \delta y} = \frac{\begin{vmatrix} 1 - \frac{u}{a} & 0 & 1 - \frac{v}{a} \\ \frac{dx}{0} & \frac{du}{dv} & \frac{0}{dy} \\ \frac{1}{a} & -\frac{1}{a} & \frac{1}{a} \end{vmatrix}}{\begin{vmatrix} u & 2uv & v \\ \frac{dx}{u} & \frac{du}{2uv} & \frac{0}{v} \\ 0 & dv & dy \end{vmatrix}} \quad (4.5)$$

When the numerator and denominator both equal zero, 17 is indeterminate along two characteristic lines. To find the directions of these characteristic lines, the denominator

determinant is set to zero and solved for $\frac{1}{1}$, resulting in equation 4.6 below. Replacing u with

$V \cos \theta$ and v with $V \sin \theta$ and substituting speed of sound with the local Mach angle turns equation 4.6 into equation 4.7.

$$\frac{dy}{dx} = \frac{-\frac{uv}{a} \mp \sqrt{\frac{u+v}{a}-1}}{1 - \frac{u}{a}} \quad (4.6)$$

$$\frac{dy}{dx} = \tan(\theta \mp \mu) \quad (4.7)$$

Equation 4.7 states that at a given point A in the nozzle, there exists two characteristic lines. The line angled upwards is the left-running C_+ characteristic and the line angled downwards is the right-running C_- characteristic.

After finding the directions of the characteristic lines, it is necessary to determine the governing compatibility equations that hold along those lines, accomplished by setting the numerator in equation 4.5 to zero and turning it into equation 4.8.

$$\frac{dv}{du} = \frac{-1 - \frac{u}{a}}{1 - \frac{v}{a}} \frac{dy}{dx} \quad (4.8)$$

Substituting equation 4.6 into equation 4.8 results in

$$\frac{dv}{du} = \frac{\frac{uv}{a} \mp \sqrt{\frac{u+v}{a}-1}}{1 - \frac{v}{a}} \quad (4.9)$$

Replacing u with $V \cos \theta$ and v with $V \sin \theta$ and substituting speed of sound with the local Mach angle turns equation 4.9 into equation 4.10.

$$d\theta = \mp \frac{1}{M-1} \frac{dV}{V} \quad (4.10)$$

Integrating equation 4.9 results in two equations in terms of the Prandtl-Meyer function.

$$\theta + \nu(M) = K \quad (4.11)$$

$$\theta - \nu(M) = K \quad (4.12)$$

Equations 4.11 and 4.12 state that the K_- value along any C_- characteristic and the K_+ value along any C_+ characteristic are constant. Knowing K_- and K_+ at any given point results in the same K_- value along the C_- characteristic and the same K_+ value along the C_+ characteristic.

4.2 Method of Characteristics: Application

It was decided to use ten characteristic lines to design the contour of the nozzle. This strikes a balance between ease of calculation and retains some accuracy, though in reality, there are an infinite number of characteristic lines in a nozzle. From the previous chapter, the final nozzle has an exit height of 4 inches and a throat height of 0.9445 inches. This is halved to 4 and 0.4722 inches respectively for a symmetric nozzle. The ten lines start at the throat, above the contour of the nozzle and are angled to intersect it to form an arc with a radius of curvature of 0.25 inches. This gradual expansion ensures that the flow coming from the converging section does not separate when it reaches the throat. The ten characteristic lines form a total of 75 points, starting from the 10 points on the gradual expansion section and continuing on each C_+ characteristic line.

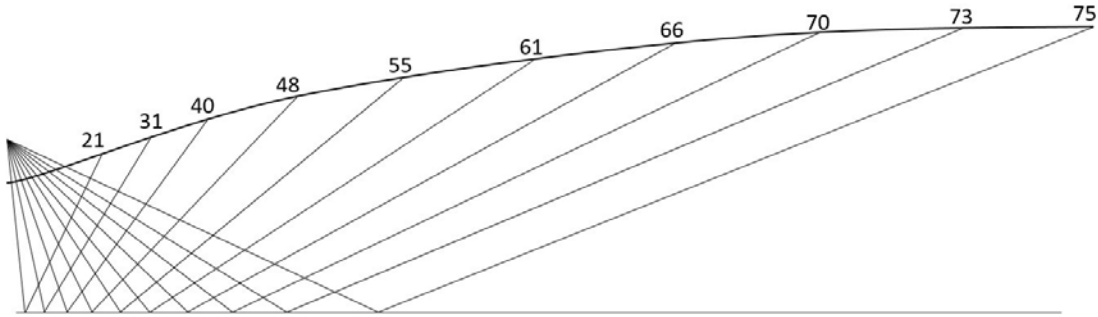


Figure 4.1 Preliminary Method of Characteristics with Wall Points

Points 1 through 10 form the gradual expansion section while points 21, 31, 40, 48, 55, 61, 66, 70, 73, and 75 serve to straighten the flow to allow it to become uniform at the exit. Points 11, 22, 32, 41, 49, 56, 62, 67, 71, and 74 form the axis of symmetry.

The θ of the first characteristic line passing through points 1 and 2 was chosen to be a very small value of 0.00183. This allowed point 21, which is at the end of the reflected line, to be located as close as possible to point 10, ensuring that the final contour stays as true as possible to a contour of infinite characteristic lines. This concept is shown in figure 4.2 below.

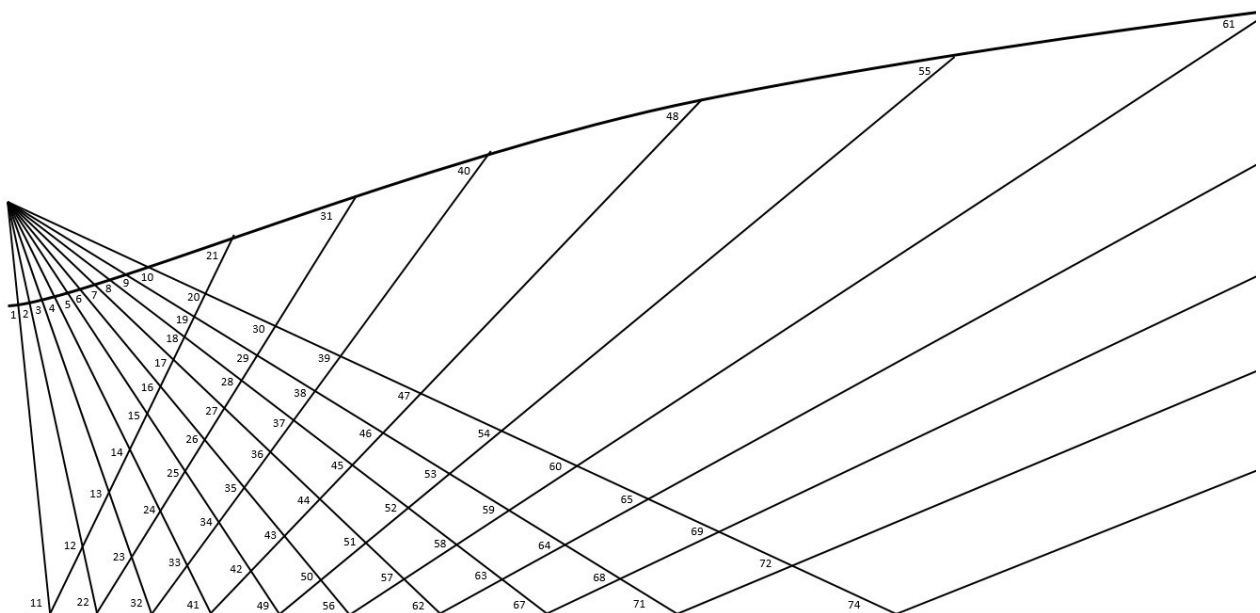


Figure 4.2 Preliminary Method of Characteristics with Labeled Points

From the desired final Mach number of three, a v of 49.76 was achieved. This caused the θ of point 10, which has the highest θ value, to be 24.88. With the θ at points 1 and 10 finalized, the θ values of points 2 through 9 are set such that there is a constant change in θ from point 1 to 10. With the points along the axis of symmetry set at zero, the rest of the points can be calculated using K_+ and K_- . Trigonometric equations are used to determine the x and y coordinates.

Table 4.1 10-Line Method of Characteristics. The wall points are highlighted in yellow.

Point	$K_- = \theta + v$	$K_+ = \theta - v$	θ (deg)	v	M	μ (deg)	x	y
1	0.004	0.000	0.002	0.002	1.001	87.215	0.000	0.472
2	5.528	0.000	2.764	2.764	1.167	58.986	0.012	0.473
3	11.057	0.000	5.528	5.528	1.276	51.582	0.024	0.473
4	16.585	0.000	8.293	8.293	1.376	46.623	0.036	0.475
5	22.114	0.000	11.057	11.057	1.471	42.823	0.048	0.477
6	27.642	0.000	13.821	13.821	1.565	39.718	0.060	0.479
7	33.171	0.000	16.585	16.585	1.658	37.083	0.071	0.483
8	38.699	0.000	19.350	19.350	1.753	34.788	0.083	0.486
9	44.228	0.000	22.114	22.114	1.848	32.753	0.094	0.491
10	49.760	0.000	24.880	24.880	1.946	30.920	0.105	0.495
11	0.004	0.000	0.002	0.002	1.001	87.215	0.000	0.000
12	5.528	0.000	2.764	2.764	1.167	58.986	0.018	0.360
13	11.057	0.000	5.528	5.528	1.276	51.582	0.032	0.387
14	16.585	0.000	8.293	8.293	1.376	46.623	0.046	0.408
15	22.114	0.000	11.057	11.057	1.471	42.823	0.058	0.425
16	27.642	0.000	13.821	13.821	1.565	39.718	0.069	0.441
17	33.171	0.000	16.585	16.585	1.658	37.083	0.080	0.455
18	38.699	0.000	19.350	19.350	1.753	34.788	0.089	0.468
19	44.228	0.000	22.114	22.114	1.848	32.753	0.098	0.480
20	49.760	0.000	24.880	24.880	1.946	30.920	0.107	0.492
21	49.760	0.000	24.880	24.880	1.946	30.920	0.111	0.498
22	5.528	-5.528	0.000	5.528	1.276	51.582	0.258	0.000
23	11.057	-5.528	2.764	8.293	1.376	46.623	0.325	0.084
24	16.585	-5.528	5.528	11.057	1.471	42.823	0.378	0.146
25	22.114	-5.528	8.293	13.821	1.565	39.718	0.424	0.198
26	27.642	-5.528	11.057	16.585	1.658	37.083	0.468	0.247
27	33.171	-5.528	13.821	19.350	1.753	34.788	0.510	0.294
28	38.699	-5.528	16.585	22.114	1.848	32.753	0.551	0.340
29	44.228	-5.528	19.350	24.878	1.946	30.921	0.592	0.388

30	49.760	-5.528	22.116	27.644	2.046	29.254	0.623	0.425
31	49.760	-5.528	22.116	27.644	2.046	29.254	1.014	0.891
32	11.057	-11.057	0.000	11.057	1.471	42.823	0.412	0.000
33	16.585	-11.057	2.764	13.821	1.565	39.718	0.483	0.066
34	22.114	-11.057	5.528	16.585	1.658	37.083	0.547	0.124
35	27.642	-11.057	8.293	19.350	1.753	34.788	0.607	0.179
36	33.171	-11.057	11.057	22.114	1.848	32.753	0.666	0.234
37	38.699	-11.057	13.821	24.878	1.946	30.921	0.724	0.290
38	44.228	-11.057	16.585	27.642	2.046	29.255	0.783	0.349
39	49.760	-11.057	19.352	30.408	2.150	27.724	0.827	0.394
40	49.760	-11.057	19.352	30.408	2.150	27.724	1.486	1.070
41	16.585	-16.585	0.000	16.585	1.658	37.083	0.570	0.000
42	22.114	-16.585	2.764	19.350	1.753	34.788	0.650	0.060
43	27.642	-16.585	5.528	22.114	1.848	32.753	0.727	0.120
44	33.171	-16.585	8.293	24.878	1.946	30.921	0.803	0.180
45	38.699	-16.585	11.057	27.642	2.046	29.255	0.880	0.242
46	44.228	-16.585	13.821	30.407	2.149	27.725	0.958	0.309
47	49.760	-16.585	16.587	33.173	2.256	26.309	1.018	0.362
48	49.760	-16.585	16.587	33.173	2.256	26.309	2.009	1.239
49	22.114	-22.114	0.000	22.114	1.848	32.753	0.746	0.000
50	27.642	-22.114	2.764	24.878	1.946	30.921	0.841	0.061
51	33.171	-22.114	5.528	27.642	2.046	29.255	0.936	0.124
52	38.699	-22.114	8.293	30.407	2.149	27.725	1.034	0.192
53	44.228	-22.114	11.057	33.171	2.256	26.310	1.135	0.265
54	49.760	-22.114	13.823	35.937	2.367	24.991	1.211	0.324
55	49.760	-22.114	13.823	35.937	2.367	24.991	2.626	1.407
56	27.642	-27.642	0.000	27.642	2.046	29.255	0.955	0.000
57	33.171	-27.642	2.764	30.407	2.149	27.725	1.071	0.065
58	38.699	-27.642	5.528	33.171	2.256	26.310	1.192	0.136
59	44.228	-27.642	8.293	35.935	2.367	24.992	1.319	0.215
60	49.760	-27.642	11.059	38.701	2.482	23.757	1.415	0.278
61	49.760	-27.642	11.059	38.701	2.482	23.757	3.374	1.572
62	33.171	-33.171	0.000	33.171	2.256	26.310	1.210	0.000
63	38.699	-33.171	2.764	35.935	2.367	24.992	1.358	0.073
64	44.228	-33.171	5.528	38.699	2.482	23.758	1.516	0.156
65	49.760	-33.171	8.295	41.465	2.603	22.597	1.635	0.223
66	49.760	-33.171	8.295	41.465	2.603	22.597	4.296	1.729
67	38.699	-38.699	0.000	38.699	2.482	23.758	1.536	0.000
68	44.228	-38.699	2.764	41.464	2.602	22.597	1.731	0.085
69	49.760	-38.699	5.530	44.230	2.729	21.500	1.878	0.155
70	49.760	-38.699	5.530	44.230	2.729	21.500	5.446	1.868

71	44.228	-44.228	0.000	44.228	2.728	21.501	1.968	0.000
72	49.760	-44.228	2.766	46.994	2.861	20.460	2.147	0.071
73	49.760	-44.228	2.766	46.994	2.861	20.460	6.894	1.973
74	49.760	-49.760	0.000	49.760	3.000	19.469	2.352	0.000
75	49.760	-49.760	0.000	49.760	3.000	19.469	8.011	2.000

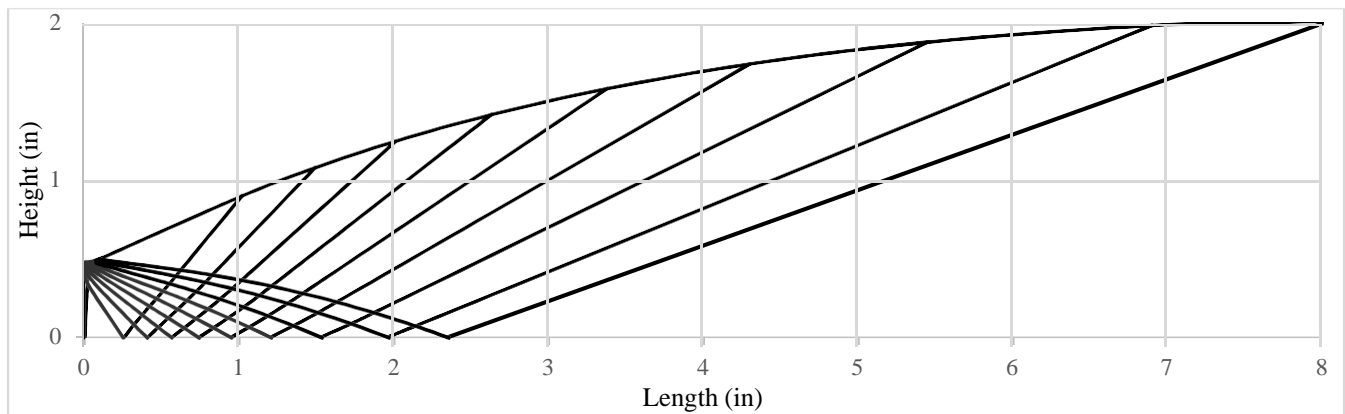


Figure 4.3 10-Line Method of Characteristics with Internal Lines

Plotting the wall points along a best-fit line results in equation 4.13, which is the equation of the contour of the nozzle. A third-order polynomial function was chosen due to the presence of an inflection point between the convex expansion section and the concave straightening section.

$$y = 0.0018x^7 - 0.0506x^5 + 0.4831x^3 + 0.456 \quad (4.13)$$

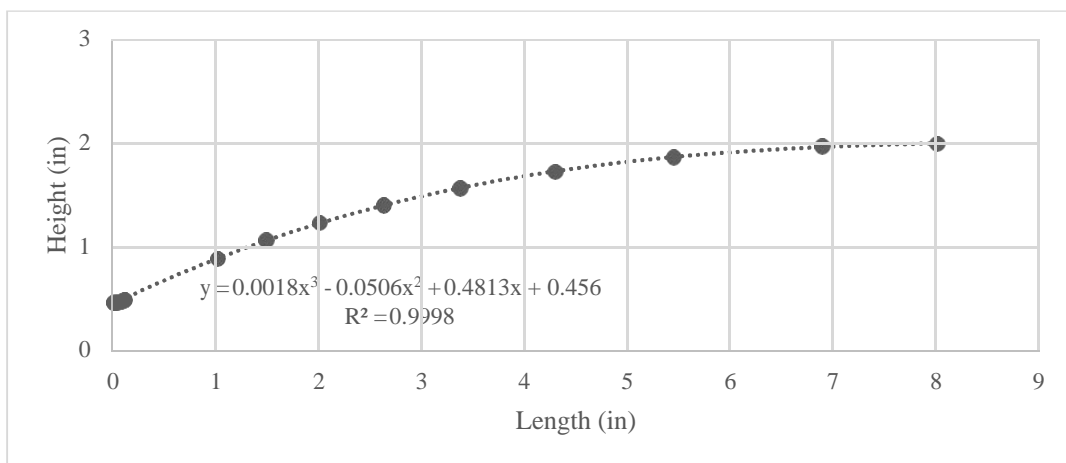


Figure 4.4 Method of Characteristics Nozzle Contour

5 CFD Analysis and Verification

After arriving at the equation for the nozzle contour, it is necessary to use CFD to verify whether the nozzle has been properly designed. A properly designed nozzle will be void of any shocks and accelerates the flow to Mach 3. Two different simulations will be run: an inviscid case and a viscous case. The inviscid simulation serves to verify that the nozzle has been properly designed. The viscous simulation models a “real-world” flow by introducing boundary layer effects and helps to predict how much of an influence the boundary layers can have on the flow. Both flows will be modeled assuming perfectly expanded conditions. The ESI suite of CFD software will be used to accomplish this.

5.1 Mesh Generation and Problem Setup

Equation 4.13 will be used to solve for y-coordinate values for every x-coordinate from 0 with a step size of 0.005 inches until a value of 2 is reached. The value of 2 corresponds to an x value of 8.85 inches. This is 0.84 inches longer than the ideal nozzle designed using the method of characteristics and is caused by equation 4.13 having an R-squared value of 0.9998 and the fact that only ten characteristic lines were used. Though it is very close to the ideal value of one, there will be some inconsistencies. Also of note is that the first height value at $x=0$ is 0.456, not the designed value of 0.472. This is also due to the previously mentioned problem and is solved by setting the first height value to 0.472 and starting equation 4.13 at $x=0.04$. Please refer to appendix D for the full list of coordinates.

All 1763 coordinate points are imported into SolidWorks to form the diverging section of the nozzle. The converging section is formed using the spline tool and ensuring that the slope at the inlet and throat are both zero. The final drawing is shown below in figure 5.1.

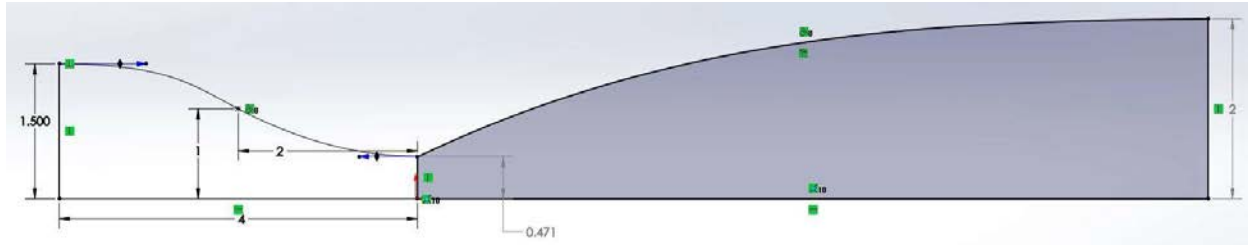


Figure 5.1 SolidWorks Drawing

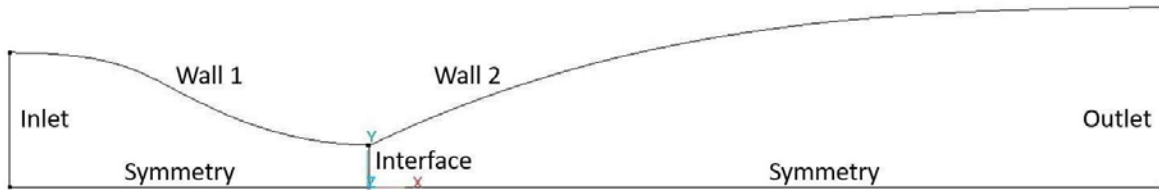


Figure 5.2 CFD-GEOM Boundary Labels

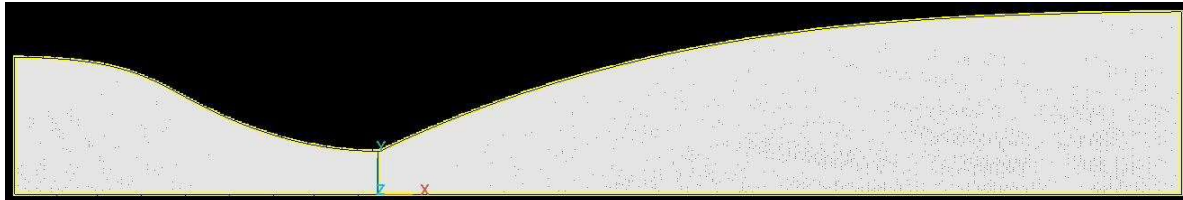


Figure 5.3 CFD-GEOM Mesh

Figure 5.1 is imported into CFD-GEOM for meshing. Wall 1 and the symmetry boundary under it are given 250 points, equally spaced. Wall 2 and the symmetry boundary under it are given 300 points, also equally spaced. The inlet, interface, and outlet boundaries are all given 500 points with a power law of two. This bias of points towards both walls helps to consolidate more cells near the walls where boundary layers may form. The smaller the cells near the wall, the more accurate the boundary layer properties can be modeled. This results in a total of 175000 nodes and 173652 cells. The final mesh in figure 5.3 is sent to CFD-FASTTRAN to setup the CFD simulation.

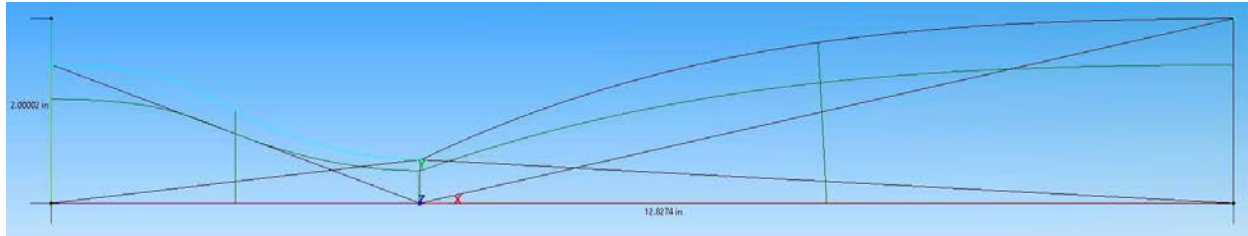


Figure 5.4 CFD-FASTRAN Model

The inviscid simulation is modeled using an ideal gas with a molecular weight of 28.97 grams per mol and a specific heat ratio of 1.4. Wall 1 and wall 2 are set as adiabatic with no flow penetration. Both symmetry boundaries and the interface are set as named. The outlet is set with a fixed static pressure of 100 Pa to create a pressure difference to start the nozzle. The inlet properties and volume initial conditions are shown below in tables 5.1 and 5.2. The simulation is set to a steady state solver with a convergence criterion of 10E-5 and started.

Table 5.1 Inviscid Inlet Boundary Conditions

Subtype	Fixed Mass Flow Rate
U (m/s)	10
V (m/s)	0
Static Pressure (Pa)	3721667.25
Static Temperature (K)	250

Table 5.2 Inviscid Volume Initial Conditions

U (m/s)	0
V (m/s)	0
Static Pressure (Pa)	101325
Static Temperature (K)	300

The viscous simulation has a similar setup but different model options and inlet boundary conditions, shown below in tables 5.3 and 5.4. Other conditions remain the same. The simulation is also set to a steady state solver but with a tighter convergence criterion of 10E-9 and started.

Table 5.3 Turbulent Model Options

Ideal Gas Molecular Weight (g/mol)	28.97
Ideal Gas Specific Heat Ratio	1.4
Viscosity Model	Sutherland's Law
Sutherland's Law "A" Coefficient (K ^{1/2} *kg/ms)	1.4605E-006
Sutherland's Law "B" Coefficient (K)	112
Conductivity Prandtl Number	0.7
Turbulent Conductivity	0.9
Turbulence Model	Menter-SST K-Omega

Table 5.4 Turbulent Inlet Boundary Conditions

Subtype	Fixed Mass Flow Rate
U (m/s)	10
V (m/s)	0
Static Pressure (Pa)	3721667.25
Static Temperature (K)	250
Turbulent Kinetic Energy (k)	0
Dissipation Rate (Omega)	0

Both inviscid and turbulent simulations use the Reynolds-averaged Navier-Stokes (RANS) equations, which are time-averaged equations for fluid flow shown below.

$$\rho \tilde{u} \frac{\delta u}{\delta t} + u \frac{\delta u}{\delta x} = - \frac{\delta p}{\delta x} + \frac{\delta T}{\delta x} \quad (5.1)$$

$$\frac{1}{\delta t} \frac{\delta \rho}{\delta t} + u \frac{\delta \rho}{\delta x} + \rho \frac{\delta u}{\delta x} = 0 \quad (5.2)$$

$\tilde{u}_i(\vec{x}, t)$ represents the i-the component of the fluid velocity at a point in space and time, t. Also $p(\vec{x}, t)$ represents the static pressure, $T(\vec{x}, t)$, the viscous stresses, and ρ the fluid density. The tilde over the symbol indicates that an instantaneous quantity is being considered [16].

However, the two equations are not closed for turbulent problems and other equations must be used. Menter's Shear Stress Transport (SST) k-omega turbulence model is a two-equation eddy-viscosity model which combines the function of both the $k - \omega$ and $k - \varepsilon$ models.

The $k - \omega$ model has a strict focus on flow near the wall while the $k - \varepsilon$ model focuses more on the free-stream flow [17]. Combining both models ensures that no part of the flow is neglected and the resulting viscous effects can be modeled with greater accuracy. The turbulent kinetic energy and specific dissipation rate equations are shown below. Please refer to appendix E for variable definitions.

$$\frac{\delta k}{\delta t} + U \frac{\delta k}{\delta x} = P - \beta^* k \omega + \frac{\delta}{\delta x} \left(\nu + \sigma \nu^7 \right) \frac{\delta k}{\delta x} \quad (5.3)$$

$$\frac{\delta \omega}{\delta t} + U \frac{\delta \omega}{\delta x} = \alpha S - \beta \omega + \frac{\delta}{\delta x} \left(\nu + \sigma \nu^7 \right) \frac{\delta \omega}{\delta x} + 2(1 - F) \sigma^7 \frac{1}{\omega} \frac{\delta k}{\delta x} \frac{\delta \omega}{\delta x} \quad (5.4)$$

5.2 Results and Discussion

5.2.1 Inviscid Simulation Results

The inviscid simulation converged to the specified tolerance after almost 90,000 iterations. The converged flow properties are mirrored about the axis of symmetry and shown below in figures 5.5 through 5.8.

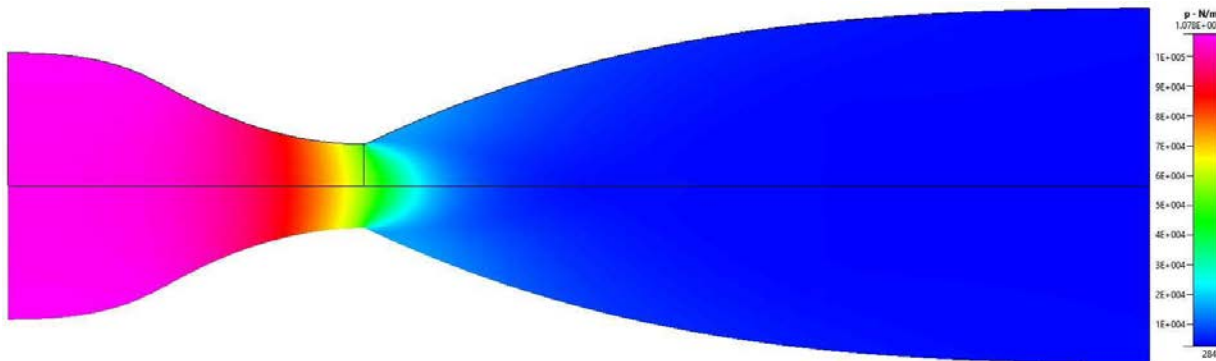


Figure 5.5 Pressure Contour of Converged Inviscid Simulation

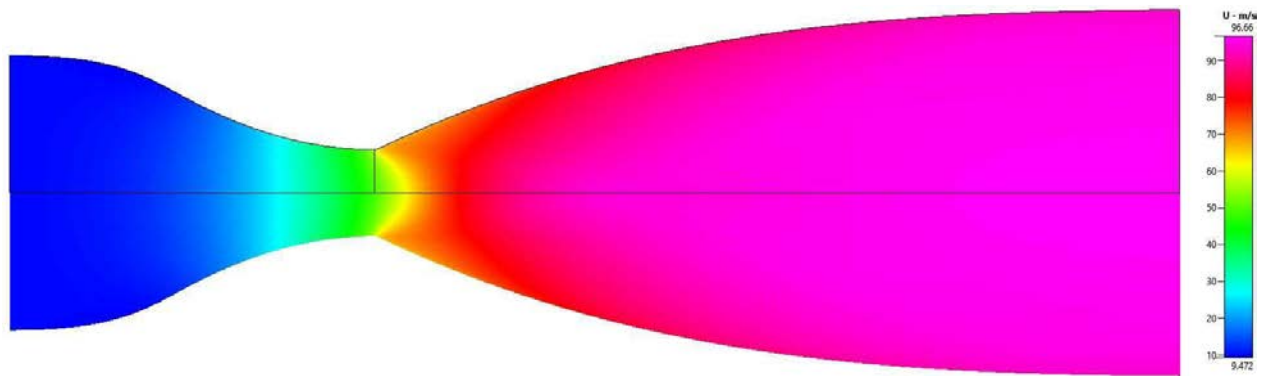


Figure 5.6 U Velocity Contour of Converged Inviscid Simulation

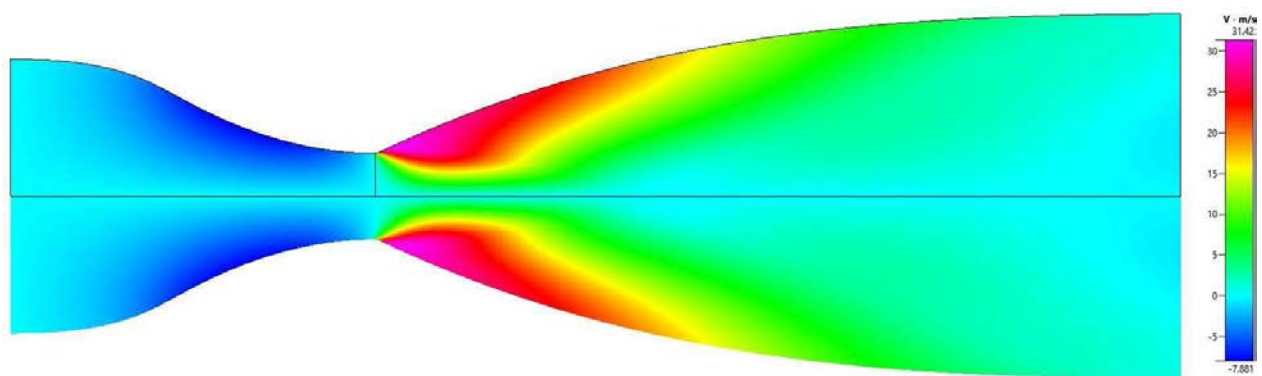


Figure 5.7 V Velocity Contour of Converged Inviscid Simulation

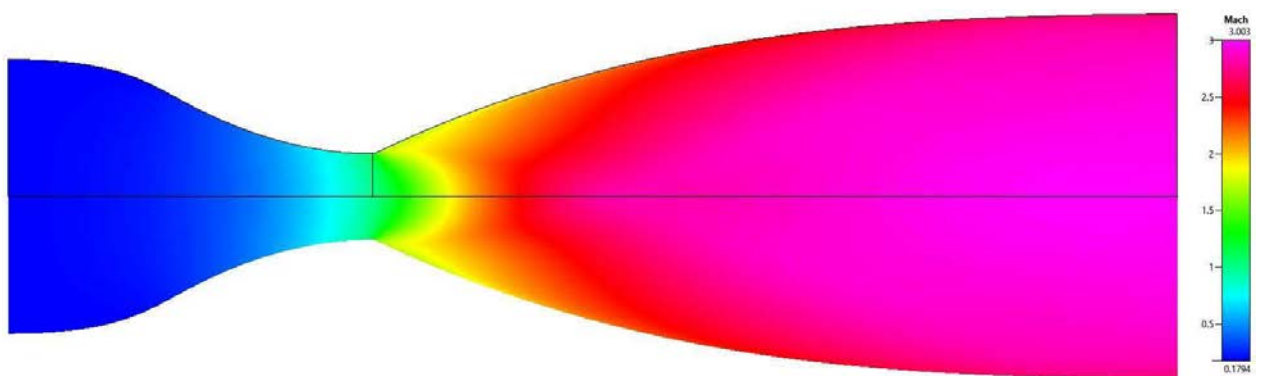


Figure 5.8 Mach Contour of Converged Inviscid Simulation

As figure 5.7 shows, the v velocity is indeed highest in the gradual expansion sections, reaching as high as 31 m/s. In the same region, figure 5.6 shows that the u velocity reaches around 75 m/s, signifying the drastic departure from the quasi one-dimensional analysis done in

chapter 2. In addition, as figure 5.8 shows, the contour designed in chapter 4 was able to accelerate the flow to Mach 3.03 successfully. The slight difference between it and the design goal of Mach 3 is due to the contour equation having an R-squared value of 0.9998 and that only ten characteristic lines were used.

5.2.2 Viscous Simulation Results

The viscous simulation converged to the specified tolerance after almost 200,000 iterations. The converged flow properties are mirrored about the axis of symmetry and shown below in figures 5.9 through 5.12.

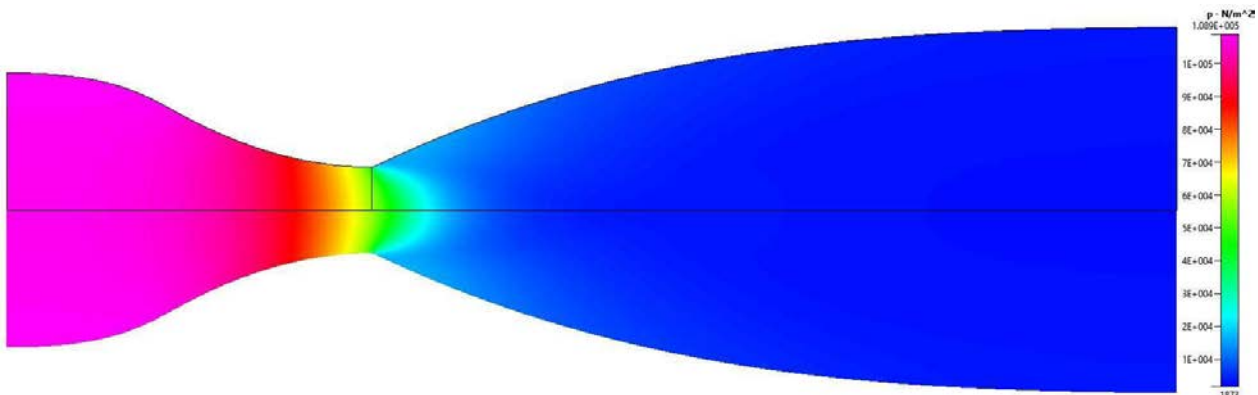


Figure 5.9 Pressure Contour of Converged Viscous Simulation

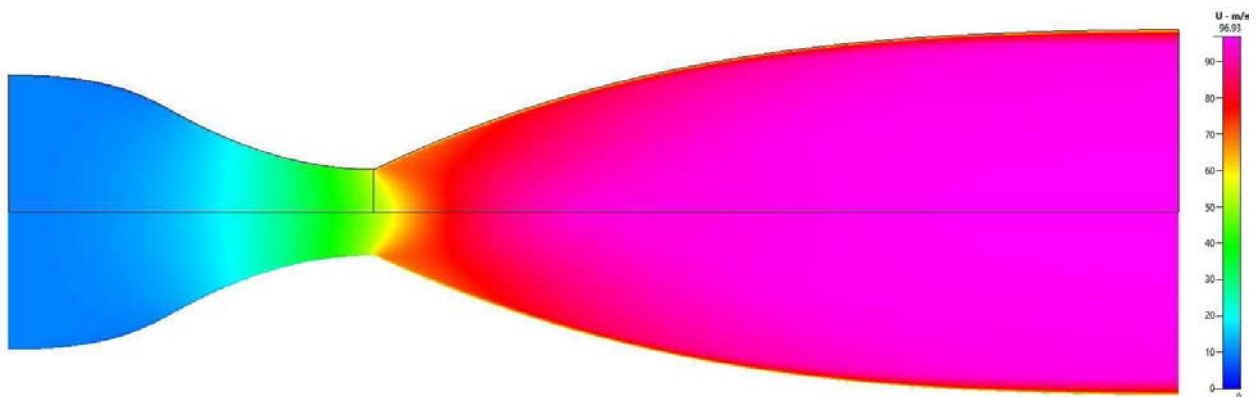


Figure 5.10 U Velocity Contour of Converged Viscous Simulation

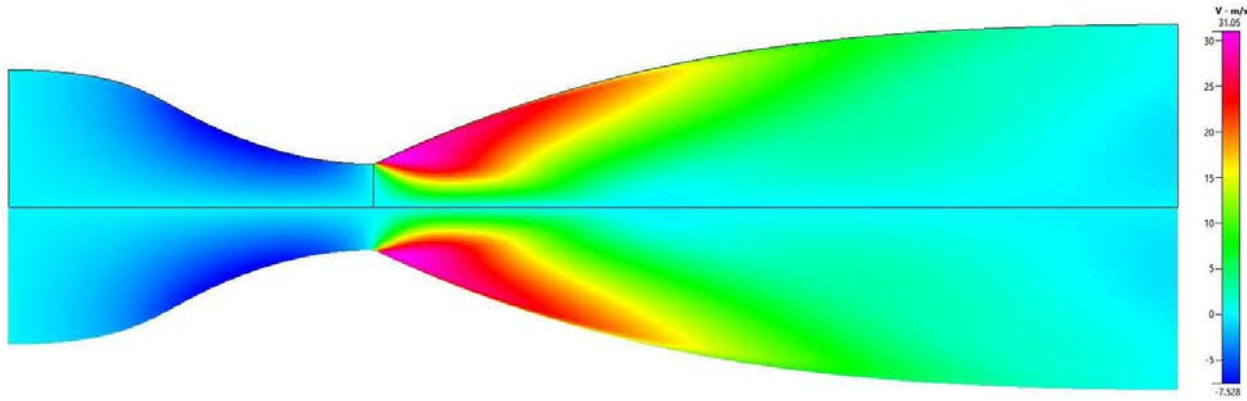


Figure 5.11 V Velocity Contour of Converged Viscous Simulation

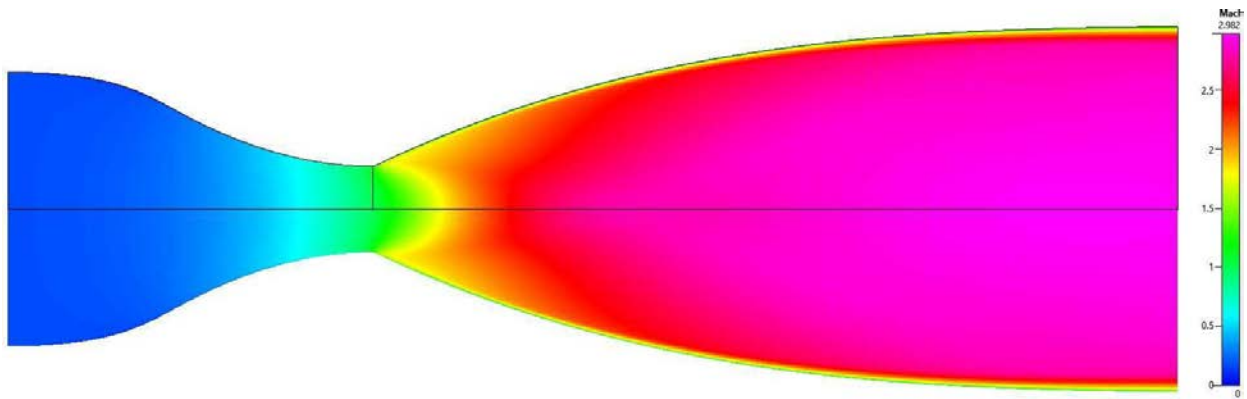


Figure 5.12 Mach Contour of Converged Viscous Simulation

As figure 5.14 shows, the appearance of boundary layers can have a profound effect on the flow properties. Boundary layers exist due to the no-slip condition imposed on the wall, stating that the layer of fluid on the surface of the wall has a velocity of zero. The layer above that is not in contact with the wall but is in contact with the layer of fluid that has a velocity of zero, slowing it down. The layers then build on top of each other, with the layer closer to the core having a velocity closer and closer to that of the core flow. The full boundary layer height is defined at the point at which the flow has a velocity that is 99% of the core flow.

Due to the turbulence within the boundary layers that grow along the wall, the inviscid area along the axis of the nozzle is reduced. According to equation 2.1, the Mach number is also

decreased. The exit Mach number was lowered from the inviscid value of 3.03 to a viscous value of 2.982. This shows that if the nozzle were to be built and ran according to the setup outlined in this report, it fails to achieve the ideal exit Mach of 3.

In addition, modifying the method of characteristics to include a gradual-expansion section naturally increased the length of the divergent nozzle. The increased flow quality more than justifies the extra length and weight of materials. However, it is interesting that the designed expansion section has an axial length of around 0.1 inches compared to the full divergent nozzle length of almost 9 inches. As can be seen in figures 5.9 through 5.12, this small increase was enough to prevent the flow exiting the convergent section from separating, ensuring high flow quality with a minimal increase in nozzle length.

In the end, Mach 2.982 is very close to Mach 3 and any changes in observations and experimental results are unlikely to be very drastic. As such, there will be no further changes to the contour of the designed nozzle.

6 Conclusion

In this study, a two-dimensional supersonic nozzle with an exit area of 16 in² and a throat area of 3.78 in² has been designed to achieve a desired flow of Mach 3. Fundamental concepts of isentropic flow was reviewed and a minimum-length nozzle contour was designed using equations for a two-dimensional method of characteristics. The design process was slightly adjusted to include a convex gradual-expansion section directly downstream of the throat to prevent flow separation. Afterwards, CFD simulations were run to confirm the validity of the designed nozzle. Inviscid simulations show an exit Mach of 3.03 while viscous simulations predict an exit Mach of 2.982. Due to the success of this project, the designed nozzle is being considered for use as part of an actual wind tunnel.

7 Future Works

Lowering the exit Mach number from 3.03 to 2.982 show that while minimal, the boundary layer does have an effect on the final flow properties. In addition, a machined two-dimensional nozzle has four corners that will likely also affect the flow. Three-dimensional CFD simulations can be run to predict what changes the flow will have. Afterwards adjustment can be made to the designed contour so that the desired exit Mach of 3 can be achieved even with turbulence on the walls and corners.

References

- ¹Norris, G. (2012, June). NASA Focuses Supersonic Effort On Low-Boom Propulsion. Aviation Week & Space Technology,. Retrieved from <http://aviationweek.com/awin/nasa-focuses-supersonic-effort-low-boom-propulsion>
- ²Norris, G. (2014, June). Boeing and Lockheed Unveil Supersonic Concepts. Aviation Week & Space Technology,. Retrieved from <http://aviationweek.com/technology/boeing-and-lockheed-unveil-supersonic-concepts>
- ³Moore, J. (2017, March 1). SUPERSONIC DESIGN IN WIND TUNNEL. AOPA. Retrieved from www.aopa.org
- ⁴Masunaga, S. (2017, February 2). Supersonic passenger jets might make a comeback, more than a decade after the last Concorde flight. Los Angeles Times,. Retrieved from www.latimes.com
- ⁵Carter, M. B., Elmiligui, A. A., Nayani, S. N., Castner, R., Bruce, W. E., IV, and Inskeep, J., "Computational and Experimental Study of Supersonic Nozzle Flow and Shock Interactions," NF1676L-20178, Jan 2015.
- ⁶Zebbiche, T., and Youbi, Z., "Supersonic Two-Dimensional Minimum Length Nozzle Design at High Temperature. Application for Air," Chinese Journal of Aeronautics, Vol. 20, No. 1, 2007; pp. 29-39.
DOI: 10.1016/S1000-9361(07)60004-1
- ⁷Papamoschou, D., Zill, A., Johnson, A., "Supersonic flow separation in planar nozzles," Shock Waves, Vol. 19, No. 3, 2009; pp. 171-183.
DOI 10.1007/s00193-008-0160-z
- ⁸Mon, K. O., Lee, C., "Optimal design of supersonic nozzle contour for altitude test facility," Journal of Mechanical Science and Technology, Vol. 26, No. 8, 2012; pp. 2589-2594.
DOI 10.1007/s12206-012-0634-x
- ⁹Khan, M. A., Sardiwal, S. K., Sharath, M. V. S., and Chowdary, D. H., "Design of a Supersonic Nozzle using Method of Characteristics," International Journal of Engineering Research & Technology, Vol. 2, No. 11, 2013; pp. 19-24.
- ¹⁰Beckwith, I. E., and Moore, J. A., "An accurate and rapid method for the design of supersonic nozzles," NACA-TN-3322, Feb 1955.
- ¹¹Evard, J. C., Marcus, L. R., "Achievement of continuous wall curvature in design of two-dimensional symmetrical supersonic nozzles," NACA-TN-2616, Jan 1952.
- ¹²Pinkel, I. I., "Equations for the Design of Two-dimensional Supersonic Nozzles," NACA-RM-E8B02, Jun 1948.
- ¹³Crown, J. C., "Supersonic nozzle design," NACA-TN-1651, Jun 1948.
- ¹⁴McCabe, A., "Design of a Supersonic Nozzle," R. & M. NO. 3440, Mar 1964
- ¹⁵Anderson, J. D. Jr., "Compressible Flow through Nozzles, Diffusers, and Wind Tunnels," Fundamentals of Aerodynamics, 5th ed., McGraw-Hill, New York, 2011, pp. 681-696
- ¹⁶Introduction to turbulence/Reynolds averaged equations, CFD Online, URL: <https://www.cfd-online.com/Wiki/Introduction_to_turbulence/Reynolds_averaged_equations>, retrieved May 21, 2018.
- ¹⁷SST k-omega model, CFD Online, URL: <https://www.cfd-online.com/Wiki/SST_k-omega_model>, retrieved May 19, 2018.
- ¹⁸SST (Menter's Shear Stress Transport), Wikipedia, URL: <[https://en.wikipedia.org/wiki/SST_\(Menter%20Shear_Stress_Transport\)](https://en.wikipedia.org/wiki/SST_(Menter%20Shear_Stress_Transport))>, retrieved May 21, 2018

Appendix A: Reduced Order Model MATLAB Code

```
% Yousheng Deng
% AE 295A

%% Main
clear all;
close all;
format short;
clc

% Givens
gamma = 1.4; %air
pb = 1; %back pressure atm
p0 = 20.5428; %reservoir pressure atm
syms ma;
% cp = 1.005;
% R = 0.2869;

% Geometry
radius = zeros(1,101);
length = length(radius);

for i=1:((length-1)/4)+1
    radius(1,i) = (-i+31)/5;
end

for i=((length-1)/4)+2:length
    radius(1,i) = (4*i-29)/75;
end

[radius_th,index_th] = min(radius);

areas = zeros(1,length);

for i=1:length
    areas(1,i) = radius(1,i)*radius(1,i)*pi;
end

ae = areas(end);

ar = zeros(1,length);
for i=1:length
    ar(1,i) = areas(1,i)/min(areas);
end

% Calculations
p_th = pp0(1,gamma)*p0;

ar_new = areas/(min(areas)*.15);

m_sub = maas(ar,gamma,3);
```

```

pr_sub = pp0(m_sub,gamma);

m_sup = maas(ar,gamma,4);
pr_sup = pp0(m_sup,gamma);

pes = zeros(1,length);
m_sub_sh = pes;

%iterate location of normal shock
for i=index_th+1:length
    m1 = m_sup(1,i);
    m2_ew = sqrt(((1+((gamma-1)/2)*m1^2)/(gamma*m1^2-((gamma-1)/2)));
    at_new = areas(1,i)/sqrt((1/m2_ew^2)*((2/(gamma+1))*(1+((gamma-1)/2)*m2_ew^2))^(gamma+1)/(gamma-1));
    m_sub_sh(1,i) = maas(ae/at_new,gamma,3);
    p1p2 = 1/(1+((2*gamma)/(gamma+1))*((m1^2)-1)); %Fundamentals pg 577
    p01p1 = (1+((gamma-1)/2)*(m1^2))^(gamma/(gamma-1)); %Fundamentals pg 591
    p2p02 = 1/(1+((gamma-1)/2)*(m2_ew^2))^(gamma/(gamma-1)); %Fundamentals pg 591
    p01p02 = p01p1*p1p2*p2p02;
    pes(1,i) = p0/p01p02/((1+((gamma-1)/2)*m_sub_sh(1,i)^2))^(gamma/(gamma-1));
end

[delta_p,index_sh] = min(abs(pes(index_th+1:length)-pb));
index_sh = index_sh+index_th
pe = pes(1,index_sh)
delta_p

% Calculations with Shock
ar_sh1 = ar(1,1:index_sh);
ar_sh2 = ar(1,index_sh:length);
m_sup_sh1 = maas(ar_sh1,gamma,4);
pr_sup_sh1 = pp0(m_sup_sh1,gamma);
m_sh = m_sup_sh1(1,index_sh);
% t2t1 = (1+((2*gamma)/(gamma+1))*((m_sh^2)-1))^(2+((gamma-1)*m_sh^2)/((gamma+1)*m_sh^2));
% p2p1 = (1+((2*gamma)/(gamma+1))*((m_sh^2)-1));
% ds = cp*log(t2t1)-R*log(p2p1);
% p02p01 = exp(-ds/R);

m_sup_sh = sqrt((1+((gamma-1)/2)*m_sup_sh1(1,index_sh)^2)/(gamma*m_sup_sh1(1,index_sh)^2-((gamma-1)/2))); %Mach after shock
at_sh = areas(1,index_sh)/sqrt((1/m_sup_sh^2)*((2/(gamma+1))*(1+((gamma-1)/2)*m_sup_sh^2))^(gamma+1)/(gamma-1));
ar_sh = areas/at_sh; %New area ratios
m_sup_sh2 = maas(ar_sh,gamma,3); %Machs after shock
p1p2 = 1/(1+((2*gamma)/(gamma+1))*((m_sh^2)-1));
p01p1 = (1+((gamma-1)/2)*(m_sh^2))^(gamma/(gamma-1));
p2p02 = 1/(1+((gamma-1)/2)*(m_sup_sh^2))^(gamma/(gamma-1));
p01p02 = p01p1*p1p2*p2p02;
pr_sup_sh2 = pp0(m_sup_sh2,gamma)/p01p02; %Pressure ratios after shock

```

```

%% Plots
x = linspace(0,length-1,length);
x_sh1 = linspace(0,index_sh,index_sh);
x_sh2 = linspace(index_sh,length-1,length-index_sh+1);

% ax1 = subplot(3,3,1);
% plot(ax1,x,pr_sub,'LineWidth',3);
% yL = get(gca,'YLim');
% line([index_th-1 index_th-1],yL,'Color','r');
% title(ax1,'Subsonic')
% xlabel(ax1,'Axial Length')
% ylabel(ax1,'P/P_0')
% set(gca,'XTick',[])
%
% ax2 = subplot(3,3,4);
% plot(ax2,x,m_sub,'LineWidth',3);
% xL = get(gca,'XLim');
% line(xL,[1 1],'Color','r');
% yL = get(gca,'YLim');
% line([index_th-1 index_th-1],yL,'Color','r');
% title(ax2,'')
% xlabel(ax2,'Axial Length')
% ylabel(ax2,'Mach')
% set(gca,'XTick',[])
%
% ax3 = subplot(3,3,7);
% plot(ax3,x,ar,'LineWidth',3);
% yL = get(gca,'YLim');
% line([index_th-1 index_th-1],yL,'Color','r');
% line([index_sh index_sh],yL,'Color','g');
% title(ax3,'')
% xlabel(ax3,'Axial Length')
% ylabel(ax3,'Area Ratio')
% set(gca,'XTick',[])
%
% ax4 = subplot(3,3,2);
% plot(ax4,x,pr_sup,'LineWidth',3);
% yL = get(gca,'YLim');
% line([index_th-1 index_th-1],yL,'Color','r');
% title(ax4,'Supersonic')
% xlabel(ax4,'Axial Length')
% ylabel(ax4,'P/P_0')
% set(gca,'XTick',[])
%
% ax5 = subplot(3,3,5);
% plot(ax5,x,m_sup,'LineWidth',3);
% xL = get(gca,'XLim');
% line(xL,[1 1],'Color','r');
% yL = get(gca,'YLim');
% line([index_th-1 index_th-1],yL,'Color','r');
% title(ax5,'')
% xlabel(ax5,'Axial Length')
% ylabel(ax5,'Mach')
% set(gca,'XTick',[])
%
% ax6 = subplot(3,3,8);
% plot(ax6,x,areas,'LineWidth',3);

```

```

% yL = get(gca,'YLim');
% line([index_th-1 index_th-1],yL,'Color','r');
% line([index_sh index_sh],yL,'Color','g');
% title(ax6,'')
% xlabel(ax6,'Axial Length')
% ylabel(ax6,'Area')
% set(gca,'XTick',[])
%
% ax7 = subplot(3,3,3);
% plot(ax7,x_sh1,pr_sup_sh1,'LineWidth',3);
% yL = get(gca,'YLim');
% line([index_th-1 index_th-1],yL,'Color','r');
% line([index_sh index_sh],yL,'Color','g');
% title(ax7,'Supersonic With A Normal Shock')
% xlabel(ax7,'Axial Length')
% ylabel(ax7,'P/P_0')
% set(gca,'XTick',[])
%
% hold on
% plot(ax7,x_sh2,pr_sup_sh2(index_sh:length),'LineWidth',3);
% hold off
%
% ax8 = subplot(3,3,6);
% plot(ax8,x_sh1,m_sup_sh1,'LineWidth',3);
% xL = get(gca,'XLim');
% line(xL,[1 1],'Color','r');
% yL = get(gca,'YLim');
% line([index_th-1 index_th-1],yL,'Color','r');
% line([index_sh index_sh],yL,'Color','g');
% title(ax8,'')
% xlabel(ax8,'Axial Length')
% ylabel(ax8,'Mach')
% set(gca,'XTick',[])
%
% hold on
% plot(ax8,x_sh2,m_sup_sh2(index_sh:length),'LineWidth',3);
% xL = get(gca,'XLim');
% line(xL,[1 1],'Color','r');
% hold off
%
% ax9 = subplot(3,3,9);
% plot(ax9,x,radius,'LineWidth',3);
% yL = get(gca,'YLim');
% line([index_th-1 index_th-1],yL,'Color','r');
% line([index_sh index_sh],yL,'Color','g');
% title(ax9,'')
% xlabel(ax9,'Axial Length')
% ylabel(ax9,'Radius')
% set(gca,'XTick',[])
%
% axis([ax1,ax4,ax7],[0 length-1 0 inf]);
% axis([ax2,ax5,ax8],[0 length-1 0 5]);
% axis([ax3,ax6,ax9],[0 length-1 0 10]);

ax4 = subplot(2,2,1);
plot(ax4,x,pr_sup,'LineWidth',3);
yL = get(gca,'YLim');

```

```

line([index_th-1 index_th-1],yL,'Color','r');
line([length-1 length-1],yL,'Color','k');
title(ax4,'Supersonic')
xlabel(ax4,'Axial Length')
ylabel(ax4,'P/P_0')
set(gca,'XTick',[])

```

```

ax5 = subplot(2,2,3);
plot(ax5,x,m_sup,'LineWidth',3);
xL = get(gca,'XLim');
line(xL,[1 1],'Color','r');
yL = get(gca,'YLim');
line([index_th-1 index_th-1],yL,'Color','r');
line([length-1 length-1],yL,'Color','k');
title(ax5,'')
xlabel(ax5,'Axial Length')
ylabel(ax5,'Mach')
set(gca,'XTick',[])

```

```

ax7 = subplot(2,2,2);
plot(ax7,x_sh1,pr_sup_sh1,'LineWidth',3);
yL = get(gca,'YLim');
line([index_th-1 index_th-1],yL,'Color','r');
line([length-1 length-1],yL,'Color','k');
line([index_sh index_sh],yL,'Color','g');
title(ax7,'Supersonic With A Normal Shock')
xlabel(ax7,'Axial Length')
ylabel(ax7,'P/P_0')
set(gca,'XTick',[])

```

```

hold on
plot(ax7,x_sh2,pr_sup_sh2(index_sh:length),'LineWidth',3);
hold off

```

```

ax8 = subplot(2,2,4);
plot(ax8,x_sh1,m_sup_sh1,'LineWidth',3);
xL = get(gca,'XLim');
line(xL,[1 1],'Color','r');
yL = get(gca,'YLim');
line([index_th-1 index_th-1],yL,'Color','r');
line([length-1 length-1],yL,'Color','k');
line([index_sh index_sh],yL,'Color','g');
title(ax8,'')
xlabel(ax8,'Axial Length')
ylabel(ax8,'Mach')
set(gca,'XTick',[])

```

```

hold on
plot(ax8,x_sh2,m_sup_sh2(index_sh:length),'LineWidth',3);
xL = get(gca,'XLim');
line(xL,[1 1],'Color','r');
hold off

```

```

% axis equal
axis([ax4,ax7],[0 length*1.1 0 inf]);
axis([ax5,ax8],[0 length*1.1 0 5]);

```

```

function p = pp0(mach, gamma)
p = zeros(1,length(mach));
for i=1:length(mach)
    p(1,i) = (1/(1+((gamma-1)/2)*mach(1,i)^2))^(gamma/(gamma-1));
end
end

function m = maas(ar, gamma, s)
syms ma
m=zeros(1,length(ar));
f = zeros(12, length(ar));
for i=1:length(ar)
    f(:,i) = vpasolve(ar(1,i)^2 == (1/ma^2)*((2/(gamma+1))*(1+((gamma-1)/2)*ma^2))^(gamma+1)/(gamma-1),ma);
end
for i=1:length(ar)
    if(i < length(ar))
        if(ar(1,i) > ar(1,i+1))
            m(1,i) = f(3,i);
        else
            m(1,i) = f(s,i);
        end
    else
        m(1,i) = f(s,i);
    end
end
end

```

Appendix B: Trade Study MATLAB Code

```
% Yousheng Deng
% AE 295A

% Main
clear all;
close all;
format short;
clc

% Givens
gamma = 1.4; %air
T0 = 527; %total temperature Rankine
Vg = 660; %gallons
R = 53.35*12; %specific gas constant of dry air
pt = 300; %tank pressure psi
pb = 14.7; %ambient psi
ms = 1.5:0.1:5; %machs
ae = 8:2:16; %exit area in^2

mach = 3;
p0s = 50:5:300;

% Calculations
area_ratio = sqrt((1./(ms.^2)).*((2/(gamma+1))*(1+((gamma-1)/2)*ms.^2)).^...
    ((gamma+1)./(gamma-1))); %area ratios
for i=1:length(ae)
    for j=1:length(ms)
        area_throat(i,j) = ae(1,i)./area_ratio(1,j); %throat areas
    end
end
p01p1 = (1+((gamma-1)/2)*ms.^2).^(gamma/(gamma-1));
p2p1 = 1+((2*gamma)/(gamma+1))*(ms.^2-1);
p01p2 = p01p1./p2p1;
p0 = p01p2*pb; %plenum pressure psi
pe = p0/p01p1;
% beta = asind(sqrt(((p2p1-1)*(gamma+1))/(2*gamma))+1)./ms;
beta = asind(sqrt(((pb/pe)*(gamma+1)+(gamma-1))./(2*gamma*ms.^2)));
for i=1:length(ae)
    for j=1:length(ms)
        mdots(i,j) = 0.532*(area_throat(i,j).*p0(1,j) ...
            /sqrt(T0)); %mass flow rate lbm/s
        times(i,j) = ((pt-p0(1,j))*231*Vg)./(mdots(i,j)*R*T0); %runtime s
    end
end
aas_m = sqrt((1/(mach^2))*((2/(gamma+1))*(1+((gamma-1)/2)*mach^2)).^...
    ((gamma+1)./(gamma-1))); %area ratios
for i=1:length(ae)
    ats_m(i,:) = ae(1,i)/aas_m; %throat areas
    for j=1:length(p0s)
        mdots_m(i,j) = 0.532*(ats_m(i,1).*p0s(1,j) ...
            /sqrt(T0)); %mass flow rate lbm/s
    end
end
```

```

times_m(i,j) = ((pt-p0s(1,j))*231*Vg)./(mdots_m(i,j)*R*T0); %runtime
s
end
p01p1_m = (1+((gamma-1)/2)*mach^2)^(gamma/(gamma-1));
pe_m = p0s/p01p1_m;
betas_m = asind(sqrt(((pb./pe_m)-1)*(gamma+1)/(2*gamma))+1)/mach;
for i=1:length(ae)
    for j=1:length(betas_m)
        shock_lengths(i,j) = (sqrt(ae(1,i))/2)/(2*tand(betas_m(1,j)));
    end
end

%% Plots
figure(1)
hold on
plot(ms,times(1,:), 'r', 'LineWidth',3)
plot(ms,times(2,:), 'b', 'LineWidth',3)
plot(ms,times(3,:), 'k', 'LineWidth',3)
plot(ms,times(4,:), 'g', 'LineWidth',3)
plot(ms,times(5,:), 'm', 'LineWidth',3)
hold off
% title('Runtimes with Overexpanded Flow')
xlabel('Mach')
ylabel('Runtime (s)')
legend('Exit Area = 8 in^2', 'Exit Area = 10 in^2', 'Exit Area = 12 in^2',...
    'Exit Area = 14 in^2', 'Exit Area = 16 in^2')
set(gca,'FontSize',20)

figure(2)
hold on
plot(p0s,times_m(1,:), 'r', 'LineWidth',3)
plot(p0s,times_m(2,:), 'b', 'LineWidth',3)
plot(p0s,times_m(3,:), 'k', 'LineWidth',3)
plot(p0s,times_m(4,:), 'g', 'LineWidth',3)
plot(p0s,times_m(5,:), 'm', 'LineWidth',3)
hold off
% title('Runtimes for Mach 3 Flow at Various Plenum Pressures')
xlabel('Plenum Pressure (psi)')
ylabel('Runtime (s)')
legend('Exit Area = 8 in^2', 'Exit Area = 10 in^2', 'Exit Area = 12 in^2',...
    'Exit Area = 14 in^2', 'Exit Area = 16 in^2')
set(gca,'FontSize',20)
axis([180 inf 0 7]);

figure(3)
hold on
plot(p0s,shock_lengths(1,:), 'r', 'LineWidth',3)
plot(p0s,shock_lengths(2,:), 'b', 'LineWidth',3)
plot(p0s,shock_lengths(3,:), 'k', 'LineWidth',3)
plot(p0s,shock_lengths(4,:), 'g', 'LineWidth',3)
plot(p0s,shock_lengths(5,:), 'm', 'LineWidth',3)
hold off
% title('Shock Lengths for Mach 3 Flow at Various Plenum Pressures')
xlabel('Plenum Pressure (psi)')
ylabel('Shock Length (in)')

```

```

legend('Exit Area = 8 in^2', 'Exit Area = 10 in^2', 'Exit Area = 12 in^2',...
       'Exit Area = 14 in^2', 'Exit Area = 16 in^2')
set(gca, 'FontSize', 20)
axis([180 inf 0.5 3]);

figure(4)
hold on
plot(times_m(1,:),shock_lengths(1,:),'r','LineWidth',3)
plot(times_m(2,:),shock_lengths(2,:),'b','LineWidth',3)
plot(times_m(3,:),shock_lengths(3,:),'k','LineWidth',3)
plot(times_m(4,:),shock_lengths(4,:),'g','LineWidth',3)
plot(times_m(5,:),shock_lengths(5,:),'m','LineWidth',3)
hold off
% title('Shock Lengths vs Runtimes for Mach 3 Flow at Various Constant Exit Areas')
xlabel('Runtimes (s)')
ylabel('Shock Length (in)')
legend('Exit Area = 8 in^2', 'Exit Area = 10 in^2', 'Exit Area = 12 in^2',...
       'Exit Area = 14 in^2', 'Exit Area = 16 in^2')
set(gca, 'FontSize', 20)
axis([0 12 0.8 2.2]);

```

Appendix C: Method of Characteristics

Point	$K_- = \theta + v$	$K_+ = \theta - v$	θ (deg)	v	M	μ (deg)
1	0.004	0	0.002	0.002	1.001	87.215
2	5.528	0	2.764	2.764	1.167	58.986
3	11.057	0	5.528	5.528	1.276	51.582
4	16.585	0	8.293	8.293	1.376	46.623
5	22.114	0	11.057	11.057	1.471	42.823
6	27.642	0	13.821	13.821	1.565	39.718
7	33.171	0	16.585	16.585	1.658	37.083
8	38.699	0	19.350	19.350	1.753	34.788
9	44.228	0	22.114	22.114	1.848	32.753
10	49.760	0	24.880	24.880	1.946	30.920
11	0.004	0	0.002	0.002	1.001	87.215
12	5.528	0	2.764	2.764	1.167	58.986
13	11.057	0	5.528	5.528	1.276	51.582
14	16.585	0	8.293	8.293	1.376	46.623
15	22.114	0	11.057	11.057	1.471	42.823
16	27.642	0	13.821	13.821	1.565	39.718
17	33.171	0	16.585	16.585	1.658	37.083
18	38.699	0	19.350	19.350	1.753	34.788
19	44.228	0	22.114	22.114	1.848	32.753
20	49.760	0	24.880	24.880	1.946	30.920
21	49.760	0	24.880	24.880	1.946	30.920
22	5.528	-5.528	0	5.528	1.276	51.582
23	11.057	-5.528	2.764	8.293	1.376	46.623
24	16.585	-5.528	5.528	11.057	1.471	42.823
25	22.114	-5.528	8.293	13.821	1.565	39.718
26	27.642	-5.528	11.057	16.585	1.658	37.083
27	33.171	-5.528	13.821	19.350	1.753	34.788
28	38.699	-5.528	16.585	22.114	1.848	32.753
29	44.228	-5.528	19.350	24.878	1.946	30.921
30	49.760	-5.528	22.116	27.644	2.046	29.254
31	49.760	-5.528	22.116	27.644	2.046	29.254
32	11.057	-11.057	0	11.057	1.471	42.823
33	16.585	-11.057	2.764	13.821	1.565	39.718
34	22.114	-11.057	5.528	16.585	1.658	37.083
35	27.642	-11.057	8.293	19.350	1.753	34.788
36	33.171	-11.057	11.057	22.114	1.848	32.753
37	38.699	-11.057	13.821	24.878	1.946	30.921

38	44.228	-11.057	16.585	27.642	2.046	29.255
39	49.760	-11.057	19.352	30.408	2.150	27.724
40	49.760	-11.057	19.352	30.408	2.150	27.724
41	16.585	-16.585	0	16.585	1.658	37.083
42	22.114	-16.585	2.764	19.350	1.753	34.788
43	27.642	-16.585	5.528	22.114	1.848	32.753
44	33.171	-16.585	8.293	24.878	1.946	30.921
45	38.699	-16.585	11.057	27.642	2.046	29.255
46	44.228	-16.585	13.821	30.407	2.149	27.725
47	49.760	-16.585	16.587	33.173	2.256	26.309
48	49.760	-16.585	16.587	33.173	2.256	26.309
49	22.114	-22.114	0	22.114	1.848	32.753
50	27.642	-22.114	2.764	24.878	1.946	30.921
51	33.171	-22.114	5.528	27.642	2.046	29.255
52	38.699	-22.114	8.293	30.407	2.149	27.725
53	44.228	-22.114	11.057	33.171	2.256	26.310
54	49.760	-22.114	13.823	35.937	2.367	24.991
55	49.760	-22.114	13.823	35.937	2.367	24.991
56	27.642	-27.642	0	27.642	2.046	29.255
57	33.171	-27.642	2.764	30.407	2.149	27.725
58	38.699	-27.642	5.528	33.171	2.256	26.310
59	44.228	-27.642	8.293	35.935	2.367	24.992
60	49.760	-27.642	11.059	38.701	2.482	23.757
61	49.760	-27.642	11.059	38.701	2.482	23.757
62	33.171	-33.171	0	33.171	2.256	26.310
63	38.699	-33.171	2.764	35.935	2.367	24.992
64	44.228	-33.171	5.528	38.699	2.482	23.758
65	49.760	-33.171	8.295	41.465	2.603	22.597
66	49.760	-33.171	8.295	41.465	2.603	22.597
67	38.699	-38.699	0	38.699	2.482	23.758
68	44.228	-38.699	2.764	41.464	2.602	22.597
69	49.760	-38.699	5.530	44.230	2.729	21.500
70	49.760	-38.699	5.530	44.230	2.729	21.500
71	44.228	-44.228	0	44.228	2.728	21.501
72	49.760	-44.228	2.766	46.994	2.861	20.460
73	49.760	-44.228	2.766	46.994	2.861	20.460
74	49.760	-49.760	0	49.760	3	19.469
75	49.760	-49.760	0	49.760	3	19.469

Point	Previous Point	Next Point	Ave Theta Before	Before +	Before -	Ave Theta After	After +	After -	x	y
1									0.000	0.472
2									0.012	0.473
3									0.024	0.473
4									0.036	0.475
5									0.048	0.477
6									0.060	0.479
7									0.071	0.483
8									0.083	0.486
9									0.094	0.491
10		21				24.880	55.800	-6.040	0.105	0.495
11		22				0.001	87.215	-87.214	0.000	0.000
12		23				2.764	61.750	-56.222	0.018	0.360
13		24				5.528	57.110	-46.053	0.032	0.387
14		25				8.293	54.916	-38.330	0.046	0.408
15		26				11.057	53.880	-31.766	0.058	0.425
16		27				13.821	53.540	-25.897	0.069	0.441
17		28				16.585	53.669	-20.498	0.080	0.455
18		29				19.350	54.138	-15.439	0.089	0.468
19		30				22.115	54.867	-10.638	0.098	0.480
20		31				23.498	54.418	-7.422	0.107	0.492
21		31				23.498	54.418	-7.422	0.111	0.498
22	11	32	0.001	51.583	-51.581	0.000	51.582	-51.582	0.258	0.000
23	12	33	2.764	49.387	-43.859	2.764	49.387	-43.859	0.325	0.084
24	13	34	5.528	48.351	-37.294	5.528	48.351	-37.294	0.378	0.146
25	14	35	8.293	48.011	-31.426	8.293	48.011	-31.426	0.424	0.198
26	15	36	11.057	48.140	-26.026	11.057	48.140	-26.026	0.468	0.247
27	16	37	13.821	48.610	-20.967	13.821	48.610	-20.967	0.510	0.294
28	17	38	16.585	49.338	-16.167	16.585	49.338	-16.167	0.551	0.340
29	18	39	19.350	50.271	-11.571	19.351	50.272	-11.570	0.592	0.388
30	19	40	22.115	51.369	-7.139	20.734	49.987	-8.520	0.623	0.425
31		40				20.734	49.987	-8.520	1.014	0.891
32	22	41	0	42.823	-42.823	0.000	42.823	-42.823	0.412	0.000
33	23	42	2.764	42.483	-36.954	2.764	42.483	-36.954	0.483	0.066
34	24	43	5.528	42.612	-31.555	5.528	42.612	-31.555	0.547	0.124
35	25	44	8.293	43.081	-26.496	8.293	43.081	-26.496	0.607	0.179
36	26	45	11.057	43.810	-21.696	11.057	43.810	-21.696	0.666	0.234
37	27	46	13.821	44.742	-17.100	13.821	44.742	-17.100	0.724	0.290
38	28	47	16.585	45.840	-12.669	16.586	45.841	-12.668	0.783	0.349

39	29	48	19.351	47.075	-8.373	17.969	45.693	-9.755	0.827	0.394
40		48				17.969	45.693	-9.755	1.486	1.070
41	32	49	0	37.083	-37.083	0.000	37.083	-37.083	0.570	0.000
42	33	50	2.764	37.553	-32.024	2.764	37.553	-32.024	0.650	0.060
43	34	51	5.528	38.281	-27.224	5.528	38.281	-27.224	0.727	0.120
44	35	52	8.293	39.214	-22.628	8.293	39.214	-22.628	0.803	0.180
45	36	53	11.057	40.312	-18.198	11.057	40.312	-18.198	0.880	0.242
46	37	54	13.821	41.546	-13.904	13.822	41.547	-13.903	0.958	0.309
47	38	55	16.586	42.895	-9.722	15.205	41.514	-11.104	1.018	0.362
48		55				15.205	41.514	-11.104	2.009	1.239
49	41	56	0	32.753	-32.753	0.000	32.753	-32.753	0.746	0.000
50	42	57	2.764	33.685	-28.157	2.764	33.685	-28.157	0.841	0.061
51	43	58	5.528	34.783	-23.726	5.528	34.783	-23.726	0.936	0.124
52	44	59	8.293	36.018	-19.432	8.293	36.018	-19.432	1.034	0.192
53	45	60	11.057	37.367	-15.253	11.058	37.368	-15.252	1.135	0.265
54	46	61	13.822	38.813	-11.169	12.441	37.432	-12.550	1.211	0.324
55		61				12.441	37.432	-12.550	2.626	1.407
56	49	62	0	29.255	-29.255	0.000	29.255	-29.255	0.955	0.000
57	50	63	2.764	30.489	-24.961	2.764	30.489	-24.961	1.071	0.065
58	51	64	5.528	31.838	-20.781	5.528	31.838	-20.781	1.192	0.136
59	52	65	8.293	33.285	-16.699	8.294	33.286	-16.698	1.319	0.215
60	53	66	11.058	34.815	-12.700	9.677	33.434	-14.081	1.415	0.278
61		66				9.677	33.434	-14.081	3.374	1.572
62	56	67	0	26.310	-26.310	0.000	26.310	-26.310	1.210	0.000
63	57	68	2.764	27.756	-22.228	2.764	27.756	-22.228	1.358	0.073
64	58	69	5.528	29.287	-18.230	5.529	29.288	-18.229	1.516	0.156
65	59	70	8.294	30.890	-14.303	6.912	29.509	-15.684	1.635	0.223
66		70				6.912	29.509	-15.684	4.296	1.729
67	62	71	0	23.758	-23.758	0.000	23.758	-23.758	1.536	0.000
68	63	72	2.764	25.362	-19.833	2.765	25.363	-19.832	1.731	0.085
69	64	73	5.529	27.029	-15.971	4.148	25.648	-17.352	1.878	0.155
70		73				4.148	25.648	-17.352	5.446	1.868
71	67	74	0	21.501	-21.501	0.000	21.501	-21.501	1.968	0.000
72	68	75	2.765	23.225	-17.695	1.383	21.843	-19.077	2.147	0.071
73		75				1.383	21.843	-19.077	6.894	1.973
74	71		0	19.469	-19.469	0.000	19.469	-19.469	2.352	0.000
75									8.011	2.000

Appendix D: Nozzle Contour Coordinates

X	Y	Z	X	Y	Z	X	Y	Z	X	Y	Z
0	0.472255018	0	0.315	0.602644976	0	0.6	0.7269528	0	0.885	0.843566992	0
0.04	0.475171155	0	0.32	0.604893542	0	0.605	0.729064236	0	0.89	0.845545684	0
0.045	0.477556199	0	0.325	0.607139666	0	0.61	0.731173306	0	0.895	0.847522086	0
0.05	0.479938725	0	0.33	0.609383347	0	0.615	0.73328001	0	0.9	0.8494962	0
0.055	0.482318734	0	0.335	0.611624587	0	0.62	0.73538435	0	0.905	0.851468027	0
0.06	0.484696229	0	0.34	0.613863387	0	0.625	0.737486328	0	0.91	0.853437568	0
0.065	0.487071209	0	0.345	0.61609975	0	0.63	0.739585945	0	0.915	0.855404825	0
0.07	0.489443677	0	0.35	0.618333675	0	0.635	0.741683201	0	0.92	0.857369798	0
0.075	0.491813634	0	0.355	0.620565165	0	0.64	0.743778099	0	0.925	0.859332491	0
0.08	0.494181082	0	0.36	0.622794221	0	0.645	0.74587064	0	0.93	0.861292903	0
0.085	0.49654602	0	0.365	0.625020844	0	0.65	0.747960825	0	0.935	0.863251036	0
0.09	0.498908452	0	0.37	0.627245035	0	0.655	0.750048655	0	0.94	0.865206891	0
0.095	0.501268378	0	0.375	0.629466797	0	0.66	0.752134133	0	0.945	0.867160471	0
0.1	0.5036258	0	0.38	0.63168613	0	0.665	0.754217258	0	0.95	0.869111775	0
0.105	0.505980719	0	0.385	0.633903035	0	0.67	0.756298033	0	0.955	0.871060806	0
0.11	0.508333136	0	0.39	0.636117514	0	0.675	0.758376459	0	0.96	0.873007565	0
0.115	0.510683053	0	0.395	0.638329569	0	0.68	0.760452538	0	0.965	0.874952053	0
0.12	0.51303047	0	0.4	0.6405392	0	0.685	0.762526269	0	0.97	0.876894271	0
0.125	0.515375391	0	0.405	0.642746409	0	0.69	0.764597656	0	0.975	0.878834222	0
0.13	0.517717815	0	0.41	0.644951198	0	0.695	0.766666699	0	0.98	0.880771906	0
0.135	0.520057744	0	0.415	0.647153567	0	0.7	0.7687334	0	0.985	0.882707324	0
0.14	0.522395179	0	0.42	0.649353518	0	0.705	0.77079776	0	0.99	0.884640478	0
0.145	0.524730123	0	0.425	0.651551053	0	0.71	0.77285978	0	0.995	0.88657137	0
0.15	0.527062575	0	0.43	0.653746173	0	0.715	0.774919462	0	1	0.8885	0
0.155	0.529392538	0	0.435	0.655938878	0	0.72	0.776976806	0	1.005	0.89042637	0
0.16	0.531720013	0	0.44	0.658129171	0	0.725	0.779031816	0	1.01	0.892350482	0
0.165	0.534045001	0	0.445	0.660317053	0	0.73	0.781084491	0	1.015	0.894272336	0
0.17	0.536367503	0	0.45	0.662502525	0	0.735	0.783134833	0	1.02	0.896191934	0
0.175	0.538687522	0	0.455	0.664685588	0	0.74	0.785182843	0	1.025	0.898109278	0
0.18	0.541005058	0	0.46	0.666866245	0	0.745	0.787228524	0	1.03	0.900024369	0
0.185	0.543320112	0	0.465	0.669044495	0	0.75	0.789271875	0	1.035	0.901937207	0
0.19	0.545632686	0	0.47	0.671220341	0	0.755	0.791312899	0	1.04	0.903847795	0
0.195	0.547942782	0	0.475	0.673393784	0	0.76	0.793351597	0	1.045	0.905756134	0
0.2	0.5502504	0	0.48	0.675564826	0	0.765	0.79538797	0	1.05	0.907662225	0
0.205	0.552555542	0	0.485	0.677733466	0	0.77	0.797422019	0	1.055	0.909566069	0
0.21	0.55485821	0	0.49	0.679899708	0	0.775	0.799453747	0	1.06	0.911467669	0
0.215	0.557158404	0	0.495	0.682063552	0	0.78	0.801483154	0	1.065	0.913367024	0
0.22	0.559456126	0	0.5	0.684225	0	0.785	0.803510241	0	1.07	0.915264137	0
0.225	0.561751378	0	0.505	0.686384053	0	0.79	0.80553501	0	1.075	0.917159009	0
0.23	0.564044161	0	0.51	0.688540712	0	0.795	0.807557463	0	1.08	0.919051642	0
0.235	0.566334475	0	0.515	0.690694979	0	0.8	0.8095776	0	1.085	0.920942035	0
0.24	0.568622323	0	0.52	0.692846854	0	0.805	0.811595423	0	1.09	0.922830192	0
0.245	0.570907706	0	0.525	0.694996341	0	0.81	0.813610934	0	1.095	0.924716113	0
0.25	0.573190625	0	0.53	0.697143439	0	0.815	0.815624133	0	1.1	0.9265998	0
0.255	0.575471081	0	0.535	0.69928815	0	0.82	0.817635022	0	1.105	0.928481254	0
0.26	0.577749077	0	0.54	0.701430475	0	0.825	0.819643603	0	1.11	0.930360476	0
0.265	0.580024612	0	0.545	0.703570417	0	0.83	0.821649877	0	1.115	0.932237468	0
0.27	0.582297689	0	0.55	0.705707975	0	0.835	0.823653844	0	1.12	0.93411223	0
0.275	0.584568309	0	0.555	0.707843152	0	0.84	0.825655507	0	1.125	0.935984766	0
0.28	0.586836474	0	0.56	0.709975949	0	0.845	0.827654867	0	1.13	0.937855075	0
0.285	0.589102183	0	0.565	0.712106367	0	0.85	0.829651925	0	1.135	0.939723159	0
0.29	0.59136544	0	0.57	0.714234407	0	0.855	0.831646682	0	1.14	0.941589019	0
0.295	0.593626245	0	0.575	0.716360072	0	0.86	0.833639141	0	1.145	0.943452658	0
0.3	0.5958846	0	0.58	0.718483362	0	0.865	0.835629301	0	1.15	0.945314075	0
0.305	0.598140506	0	0.585	0.720604278	0	0.87	0.837617165	0	1.155	0.947173273	0
0.31	0.600393964	0	0.59	0.722722822	0	0.875	0.839602734	0	1.16	0.949030253	0
			0.595	0.724838996	0	0.88	0.84158601	0	1.165	0.950885016	0

1.17	0.952737563	0	1.465	1.05816511	0	1.76	1.156162637	0	2.055	1.247007404	0
1.175	0.954587897	0	1.47	1.059887201	0	1.765	1.157761185	0	2.06	1.248487109	0
1.18	0.956436018	0	1.475	1.061607159	0	1.77	1.159357679	0	2.065	1.249964839	0
1.185	0.958281927	0	1.48	1.063324986	0	1.775	1.160952122	0	2.07	1.251440597	0
1.19	0.960125626	0	1.485	1.065040681	0	1.78	1.162544514	0	2.075	1.252914384	0
1.195	0.961967117	0	1.49	1.066754248	0	1.785	1.164134856	0	2.08	1.254386202	0
1.2	0.9638064	0	1.495	1.068465687	0	1.79	1.16572315	0	2.085	1.25585605	0
1.205	0.965643477	0	1.5	1.070175	0	1.795	1.167309398	0	2.09	1.257323932	0
1.21	0.96747835	0	1.505	1.071882188	0	1.8	1.1688936	0	2.095	1.258789848	0
1.215	0.969311019	0	1.51	1.073587252	0	1.805	1.170475758	0	2.1	1.2602538	0
1.22	0.971141486	0	1.515	1.075290194	0	1.81	1.172055874	0	2.105	1.261715789	0
1.225	0.972969753	0	1.52	1.076991014	0	1.815	1.173633948	0	2.11	1.263175816	0
1.23	0.974795821	0	1.525	1.078689716	0	1.82	1.175209982	0	2.115	1.264633883	0
1.235	0.97661969	0	1.53	1.080386299	0	1.825	1.176783978	0	2.12	1.26608999	0
1.24	0.978441363	0	1.535	1.082080765	0	1.83	1.178355937	0	2.125	1.267544141	0
1.245	0.980260841	0	1.54	1.083773115	0	1.835	1.179925859	0	2.13	1.268996335	0
1.25	0.982078125	0	1.545	1.085463352	0	1.84	1.181493747	0	2.135	1.270446574	0
1.255	0.983893216	0	1.55	1.087151475	0	1.845	1.183059602	0	2.14	1.271894859	0
1.26	0.985706117	0	1.555	1.088837487	0	1.85	1.184623425	0	2.145	1.273341193	0
1.265	0.987516827	0	1.56	1.090521389	0	1.855	1.186185217	0	2.15	1.274785575	0
1.27	0.989325349	0	1.565	1.092203182	0	1.86	1.187744981	0	2.155	1.276228008	0
1.275	0.991131684	0	1.57	1.093882867	0	1.865	1.189302716	0	2.16	1.277668493	0
1.28	0.992935834	0	1.575	1.095560447	0	1.87	1.190858425	0	2.165	1.279107031	0
1.285	0.994737798	0	1.58	1.097235922	0	1.875	1.192412109	0	2.17	1.280543623	0
1.29	0.996537578	0	1.585	1.098909293	0	1.88	1.19396377	0	2.175	1.281978272	0
1.295	0.99833518	0	1.59	1.100580562	0	1.885	1.195513407	0	2.18	1.283410978	0
1.3	1.0001306	0	1.595	1.102249731	0	1.89	1.197061024	0	2.185	1.284841742	0
1.305	1.001923841	0	1.6	1.1039168	0	1.895	1.198606621	0	2.19	1.286270566	0
1.31	1.003714904	0	1.605	1.105581771	0	1.9	1.2001502	0	2.195	1.287697452	0
1.315	1.005503791	0	1.61	1.107244646	0	1.905	1.201691762	0	2.2	1.2891224	0
1.32	1.007290502	0	1.615	1.108905425	0	1.91	1.203231308	0	2.205	1.290545412	0
1.325	1.009075041	0	1.62	1.11056411	0	1.915	1.20476884	0	2.21	1.29196649	0
1.33	1.010857407	0	1.625	1.112220703	0	1.92	1.206304358	0	2.215	1.293385634	0
1.335	1.012637602	0	1.63	1.113875205	0	1.925	1.207837866	0	2.22	1.294802846	0
1.34	1.014415627	0	1.635	1.115527616	0	1.93	1.209369363	0	2.225	1.296218128	0
1.345	1.016191485	0	1.64	1.117177939	0	1.935	1.210898851	0	2.23	1.297631481	0
1.35	1.017965175	0	1.645	1.118826175	0	1.94	1.212426331	0	2.235	1.299042905	0
1.355	1.0197367	0	1.65	1.120472325	0	1.945	1.213951806	0	2.24	1.300452403	0
1.36	1.021506061	0	1.655	1.12211639	0	1.95	1.215475275	0	2.245	1.301859976	0
1.365	1.023273259	0	1.66	1.123758373	0	1.955	1.216996741	0	2.25	1.303265625	0
1.37	1.025038295	0	1.665	1.125398273	0	1.96	1.218516205	0	2.255	1.304669351	0
1.375	1.026801172	0	1.67	1.127036093	0	1.965	1.220033668	0	2.26	1.306071157	0
1.38	1.02856189	0	1.675	1.128671834	0	1.97	1.221549131	0	2.265	1.307471042	0
1.385	1.03032045	0	1.68	1.130305498	0	1.975	1.223062597	0	2.27	1.308869009	0
1.39	1.032076854	0	1.685	1.131937084	0	1.98	1.224574066	0	2.275	1.310265059	0
1.395	1.033831104	0	1.69	1.133566596	0	1.985	1.226083539	0	2.28	1.311659194	0
1.4	1.0355832	0	1.695	1.135194034	0	1.99	1.227591018	0	2.285	1.313051413	0
1.405	1.037333144	0	1.7	1.1368194	0	1.995	1.229096505	0	2.29	1.31444172	0
1.41	1.039080938	0	1.705	1.138442695	0	2	1.2306	0	2.295	1.315830115	0
1.415	1.040826582	0	1.71	1.14006392	0	2.005	1.232101505	0	2.3	1.3172166	0
1.42	1.042570078	0	1.715	1.141683077	0	2.01	1.233601022	0	2.305	1.318601176	0
1.425	1.044311428	0	1.72	1.143300166	0	2.015	1.235098551	0	2.31	1.319983844	0
1.43	1.046050633	0	1.725	1.144915191	0	2.02	1.236594094	0	2.315	1.321364606	0
1.435	1.047787693	0	1.73	1.146528151	0	2.025	1.238087653	0	2.32	1.322743462	0
1.44	1.049522611	0	1.735	1.148139048	0	2.03	1.239579229	0	2.325	1.324120416	0
1.445	1.051255388	0	1.74	1.149747883	0	2.035	1.241068822	0	2.33	1.325495467	0
1.45	1.052986025	0	1.745	1.151354659	0	2.04	1.242556435	0	2.335	1.326868617	0
1.455	1.054714523	0	1.75	1.152959375	0	2.045	1.244042069	0	2.34	1.328239867	0
1.46	1.056440885	0	1.755	1.154562034	0	2.05	1.245525725	0	2.345	1.32960922	0

2.35	1.330976675	0	2.645	1.40834771	0	2.94	1.479397771	0	3.235	1.54440412	0
2.355	1.332342235	0	2.65	1.409603825	0	2.945	1.480549141	0	3.24	1.545455443	0
2.36	1.333705901	0	2.655	1.410858125	0	2.95	1.481698775	0	3.245	1.546505111	0
2.365	1.335067674	0	2.66	1.412110613	0	2.955	1.482846676	0	3.25	1.547553125	0
2.37	1.336427555	0	2.665	1.413361288	0	2.96	1.483992845	0	3.255	1.548599486	0
2.375	1.337785547	0	2.67	1.414610153	0	2.965	1.485137283	0	3.26	1.549644197	0
2.38	1.33914165	0	2.675	1.415857209	0	2.97	1.486279991	0	3.265	1.550687257	0
2.385	1.340495865	0	2.68	1.417102458	0	2.975	1.487420972	0	3.27	1.551728669	0
2.39	1.341848194	0	2.685	1.418345899	0	2.98	1.488560226	0	3.275	1.552768434	0
2.395	1.343198639	0	2.69	1.419587536	0	2.985	1.489697754	0	3.28	1.553806554	0
2.4	1.3445472	0	2.695	1.420827369	0	2.99	1.490833558	0	3.285	1.554843028	0
2.405	1.345893879	0	2.7	1.4220654	0	2.995	1.49196764	0	3.29	1.55587786	0
2.41	1.347238678	0	2.705	1.42330163	0	3	1.4931	0	3.295	1.55691105	0
2.415	1.348581597	0	2.71	1.42453606	0	3.005	1.49423064	0	3.3	1.5579426	0
2.42	1.349922638	0	2.715	1.425768692	0	3.01	1.495359562	0	3.305	1.558972511	0
2.425	1.351261803	0	2.72	1.426999526	0	3.015	1.496486766	0	3.31	1.560000784	0
2.43	1.352599093	0	2.725	1.428228566	0	3.02	1.497612254	0	3.315	1.561027421	0
2.435	1.353934508	0	2.73	1.429455811	0	3.025	1.498736028	0	3.32	1.562052422	0
2.44	1.355268051	0	2.735	1.430681263	0	3.03	1.499858089	0	3.325	1.563075791	0
2.445	1.356599723	0	2.74	1.431904923	0	3.035	1.500978437	0	3.33	1.564097527	0
2.45	1.357929525	0	2.745	1.433126794	0	3.04	1.502097075	0	3.335	1.565117632	0
2.455	1.359257458	0	2.75	1.434346875	0	3.045	1.503214004	0	3.34	1.566136107	0
2.46	1.360583525	0	2.755	1.435565169	0	3.05	1.504329225	0	3.345	1.567152955	0
2.465	1.361907725	0	2.76	1.436781677	0	3.055	1.505442739	0	3.35	1.568168175	0
2.47	1.363230061	0	2.765	1.4379964	0	3.06	1.506554549	0	3.355	1.56918177	0
2.475	1.364550534	0	2.77	1.439209339	0	3.065	1.507664654	0	3.36	1.570193741	0
2.48	1.365869146	0	2.775	1.440420497	0	3.07	1.508773057	0	3.365	1.571204089	0
2.485	1.367185896	0	2.78	1.441629874	0	3.075	1.509879759	0	3.37	1.572212815	0
2.49	1.368500788	0	2.785	1.442837471	0	3.08	1.510984762	0	3.375	1.573219922	0
2.495	1.369813822	0	2.79	1.44404329	0	3.085	1.512088065	0	3.38	1.57422541	0
2.5	1.371125	0	2.795	1.445247333	0	3.09	1.513189672	0	3.385	1.57522928	0
2.505	1.372434323	0	2.8	1.4464496	0	3.095	1.514289583	0	3.39	1.576231534	0
2.51	1.373741792	0	2.805	1.447650093	0	3.1	1.5153878	0	3.395	1.577232174	0
2.515	1.375047409	0	2.81	1.448848814	0	3.105	1.516484324	0	3.4	1.5782312	0
2.52	1.376351174	0	2.815	1.450045763	0	3.11	1.517579156	0	3.405	1.579228614	0
2.525	1.377653091	0	2.82	1.451240942	0	3.115	1.518672298	0	3.41	1.580224418	0
2.53	1.378953159	0	2.825	1.452434353	0	3.12	1.51976375	0	3.415	1.581218612	0
2.535	1.38025138	0	2.83	1.453625997	0	3.125	1.520853516	0	3.42	1.582211198	0
2.54	1.381547755	0	2.835	1.454815874	0	3.13	1.521941595	0	3.425	1.583202178	0
2.545	1.382842287	0	2.84	1.456003987	0	3.135	1.523027989	0	3.43	1.584191553	0
2.55	1.384134975	0	2.845	1.457190337	0	3.14	1.524112699	0	3.435	1.585179323	0
2.555	1.385425822	0	2.85	1.458374925	0	3.145	1.525195728	0	3.44	1.586165491	0
2.56	1.386714829	0	2.855	1.459557752	0	3.15	1.526277075	0	3.445	1.587150058	0
2.565	1.388001997	0	2.86	1.460738821	0	3.155	1.527356743	0	3.45	1.588133025	0
2.57	1.389287327	0	2.865	1.461918131	0	3.16	1.528434733	0	3.455	1.589114393	0
2.575	1.390570822	0	2.87	1.463095685	0	3.165	1.529511046	0	3.46	1.590094165	0
2.58	1.391852482	0	2.875	1.464271484	0	3.17	1.530585683	0	3.465	1.59107234	0
2.585	1.393132308	0	2.88	1.46544553	0	3.175	1.531658647	0	3.47	1.592048921	0
2.59	1.394410302	0	2.885	1.466617822	0	3.18	1.532729938	0	3.475	1.593023909	0
2.595	1.395686466	0	2.89	1.467788364	0	3.185	1.533799557	0	3.48	1.593997306	0
2.6	1.3969608	0	2.895	1.468957156	0	3.19	1.534867506	0	3.485	1.594969111	0
2.605	1.398233306	0	2.9	1.4701242	0	3.195	1.535933787	0	3.49	1.595939328	0
2.61	1.399503986	0	2.905	1.471289497	0	3.2	1.5369984	0	3.495	1.596907957	0
2.615	1.40077284	0	2.91	1.472453048	0	3.205	1.538061347	0	3.5	1.597875	0
2.62	1.40203987	0	2.915	1.473614855	0	3.21	1.53912263	0	3.505	1.598840458	0
2.625	1.403305078	0	2.92	1.474774918	0	3.215	1.540182249	0	3.51	1.599804332	0
2.63	1.404568465	0	2.925	1.475933241	0	3.22	1.541240206	0	3.515	1.600766624	0
2.635	1.405830031	0	2.93	1.477089823	0	3.225	1.542296503	0	3.52	1.601727334	0
2.64	1.407089779	0	2.935	1.478244666	0	3.23	1.543351141	0	3.525	1.602686466	0

3.53	1.603644019	0	3.825	1.657394728	0	4.12	1.70593351	0	4.415	1.749537627	0
3.535	1.604599995	0	3.83	1.658260057	0	4.125	1.706712891	0	4.42	1.750235758	0
3.54	1.605554395	0	3.835	1.659123889	0	4.13	1.707490855	0	4.425	1.750932553	0
3.545	1.606507222	0	3.84	1.659986227	0	4.135	1.708267404	0	4.43	1.751628013	0
3.55	1.607458475	0	3.845	1.660847072	0	4.14	1.709042539	0	4.435	1.752322138	0
3.555	1.608408157	0	3.85	1.661706425	0	4.145	1.709816263	0	4.44	1.753014931	0
3.56	1.609356269	0	3.855	1.662564287	0	4.15	1.710588575	0	4.445	1.753706393	0
3.565	1.610302812	0	3.86	1.663420661	0	4.155	1.711359478	0	4.45	1.754396525	0
3.57	1.611247787	0	3.865	1.664275546	0	4.16	1.712128973	0	4.455	1.755085328	0
3.575	1.612191197	0	3.87	1.665128945	0	4.165	1.712897061	0	4.46	1.755772805	0
3.58	1.613133042	0	3.875	1.665980859	0	4.17	1.713663743	0	4.465	1.756458955	0
3.585	1.614073323	0	3.88	1.66683129	0	4.175	1.714429022	0	4.47	1.757143781	0
3.59	1.615012042	0	3.885	1.667680237	0	4.18	1.715192898	0	4.475	1.757827284	0
3.595	1.615949201	0	3.89	1.668527704	0	4.185	1.715955372	0	4.48	1.758509466	0
3.6	1.6168848	0	3.895	1.669373691	0	4.19	1.716716446	0	4.485	1.759190326	0
3.605	1.617818841	0	3.9	1.6702182	0	4.195	1.717476122	0	4.49	1.759869868	0
3.61	1.618751326	0	3.905	1.671061232	0	4.2	1.7182344	0	4.495	1.760548092	0
3.615	1.619682255	0	3.91	1.671902788	0	4.205	1.718991282	0	4.5	1.761225	0
3.62	1.62061163	0	3.915	1.67274287	0	4.21	1.71974677	0	4.505	1.761900593	0
3.625	1.621539453	0	3.92	1.673581478	0	4.215	1.720500864	0	4.51	1.762574872	0
3.63	1.622465725	0	3.925	1.674418616	0	4.22	1.721253566	0	4.515	1.763247839	0
3.635	1.623390446	0	3.93	1.675254283	0	4.225	1.722004878	0	4.52	1.763919494	0
3.64	1.624313619	0	3.935	1.676088481	0	4.23	1.722754801	0	4.525	1.764589841	0
3.645	1.625235245	0	3.94	1.676921211	0	4.235	1.723503335	0	4.53	1.765258879	0
3.65	1.626155325	0	3.945	1.677752476	0	4.24	1.724250483	0	4.535	1.76592661	0
3.655	1.62707386	0	3.95	1.678582275	0	4.245	1.724996246	0	4.54	1.766593035	0
3.66	1.627990853	0	3.955	1.679410611	0	4.25	1.725740625	0	4.545	1.767258157	0
3.665	1.628906303	0	3.96	1.680237485	0	4.255	1.726483621	0	4.55	1.767921975	0
3.67	1.629820213	0	3.965	1.681062898	0	4.26	1.727225237	0	4.555	1.768584492	0
3.675	1.630732584	0	3.97	1.681886851	0	4.265	1.727965472	0	4.56	1.769245709	0
3.68	1.631643418	0	3.975	1.682709347	0	4.27	1.728704329	0	4.565	1.769905627	0
3.685	1.632552714	0	3.98	1.683530386	0	4.275	1.729441809	0	4.57	1.770564247	0
3.69	1.633460476	0	3.985	1.684349969	0	4.28	1.730177914	0	4.575	1.771221572	0
3.695	1.634366704	0	3.99	1.685168098	0	4.285	1.730912643	0	4.58	1.771877602	0
3.7	1.6352714	0	3.995	1.685984775	0	4.29	1.731646	0	4.585	1.772532338	0
3.705	1.636174565	0	4	1.6868	0	4.295	1.732377985	0	4.59	1.773185782	0
3.71	1.6370762	0	4.005	1.687613775	0	4.3	1.7331086	0	4.595	1.773837936	0
3.715	1.637976307	0	4.01	1.688426102	0	4.305	1.733837846	0	4.6	1.7744888	0
3.72	1.638874886	0	4.015	1.689236981	0	4.31	1.734565724	0	4.605	1.775138376	0
3.725	1.639771941	0	4.02	1.690046414	0	4.315	1.735292236	0	4.61	1.775786666	0
3.73	1.640667471	0	4.025	1.690854403	0	4.32	1.736017382	0	4.615	1.77643367	0
3.735	1.641561478	0	4.03	1.691660949	0	4.325	1.736741166	0	4.62	1.77707939	0
3.74	1.642453963	0	4.035	1.692466052	0	4.33	1.737463587	0	4.625	1.777723828	0
3.745	1.643344929	0	4.04	1.693269715	0	4.335	1.738184647	0	4.63	1.778366985	0
3.75	1.644234375	0	4.045	1.694071939	0	4.34	1.738904347	0	4.635	1.779008861	0
3.755	1.645122304	0	4.05	1.694872725	0	4.345	1.73962269	0	4.64	1.779649459	0
3.76	1.646008717	0	4.055	1.695672074	0	4.35	1.740339675	0	4.645	1.78028878	0
3.765	1.646893615	0	4.06	1.696469989	0	4.355	1.741055305	0	4.65	1.780926825	0
3.77	1.647776999	0	4.065	1.697266469	0	4.36	1.741769581	0	4.655	1.781563595	0
3.775	1.648658872	0	4.07	1.698061517	0	4.365	1.742482504	0	4.66	1.782199093	0
3.78	1.649539234	0	4.075	1.698855134	0	4.37	1.743194075	0	4.665	1.782833318	0
3.785	1.650418086	0	4.08	1.699647322	0	4.375	1.743904297	0	4.67	1.783466273	0
3.79	1.65129543	0	4.085	1.70043808	0	4.38	1.74461317	0	4.675	1.784097959	0
3.795	1.652171268	0	4.09	1.701227412	0	4.385	1.745320695	0	4.68	1.784728378	0
3.8	1.6530456	0	4.095	1.702015318	0	4.39	1.746026874	0	4.685	1.785357529	0
3.805	1.653918428	0	4.1	1.7028018	0	4.395	1.746731709	0	4.69	1.785985416	0
3.81	1.654789754	0	4.105	1.703586859	0	4.4	1.7474352	0	4.695	1.786612039	0
3.815	1.655659578	0	4.11	1.704370496	0	4.405	1.748137349	0	4.7	1.7872374	0
3.82	1.656527902	0	4.115	1.705152713	0	4.41	1.748838158	0	4.705	1.7878615	0

4.71	1.78848434	0	5.005	1.82305091	0	5.3	1.8535146	0	5.595	1.880152671	0
4.715	1.789105922	0	5.01	1.823600642	0	5.305	1.853997181	0	5.6	1.8805728	0
4.72	1.789726246	0	5.015	1.824149196	0	5.31	1.854478664	0	5.605	1.880991911	0
4.725	1.790345316	0	5.02	1.824696574	0	5.315	1.854959051	0	5.61	1.881410006	0
4.73	1.790963131	0	5.025	1.825242778	0	5.32	1.855438342	0	5.615	1.881827085	0
4.735	1.791579693	0	5.03	1.825787809	0	5.325	1.855916541	0	5.62	1.88224315	0
4.74	1.792195003	0	5.035	1.826331667	0	5.33	1.856393647	0	5.625	1.882658203	0
4.745	1.792809064	0	5.04	1.826874355	0	5.335	1.856869662	0	5.63	1.883072245	0
4.75	1.793421875	0	5.045	1.827415874	0	5.34	1.857344587	0	5.635	1.883485276	0
4.755	1.794033439	0	5.05	1.827956225	0	5.345	1.857818425	0	5.64	1.883897299	0
4.76	1.794643757	0	5.055	1.828495409	0	5.35	1.858291175	0	5.645	1.884308315	0
4.765	1.79525283	0	5.06	1.829033429	0	5.355	1.85876284	0	5.65	1.884718325	0
4.77	1.795860659	0	5.065	1.829570284	0	5.36	1.859233421	0	5.655	1.88512733	0
4.775	1.796467247	0	5.07	1.830105977	0	5.365	1.859702919	0	5.66	1.885535333	0
4.78	1.797072594	0	5.075	1.830640509	0	5.37	1.860171335	0	5.665	1.885942333	0
4.785	1.797676701	0	5.08	1.831173882	0	5.375	1.860638672	0	5.67	1.886348333	0
4.79	1.79827957	0	5.085	1.831706095	0	5.38	1.86110493	0	5.675	1.886753334	0
4.795	1.798881203	0	5.09	1.832237152	0	5.385	1.86157011	0	5.68	1.887157338	0
4.8	1.7994816	0	5.095	1.832767053	0	5.39	1.862034214	0	5.685	1.887560344	0
4.805	1.800080763	0	5.1	1.8332958	0	5.395	1.862497244	0	5.69	1.887962356	0
4.81	1.800678694	0	5.105	1.833823394	0	5.4	1.8629592	0	5.695	1.888363374	0
4.815	1.801275393	0	5.11	1.834349836	0	5.405	1.863420084	0	5.7	1.8887634	0
4.82	1.801870862	0	5.115	1.834875128	0	5.41	1.863879898	0	5.705	1.889162435	0
4.825	1.802465103	0	5.12	1.83539927	0	5.415	1.864338642	0	5.71	1.88956048	0
4.83	1.803058117	0	5.125	1.835922266	0	5.42	1.864796318	0	5.715	1.889957537	0
4.835	1.803649904	0	5.13	1.836444115	0	5.425	1.865252928	0	5.72	1.890353606	0
4.84	1.804240467	0	5.135	1.836964819	0	5.43	1.865708473	0	5.725	1.890748691	0
4.845	1.804829807	0	5.14	1.837484379	0	5.435	1.866162953	0	5.73	1.891142791	0
4.85	1.805417925	0	5.145	1.838002798	0	5.44	1.866616371	0	5.735	1.891535908	0
4.855	1.806004822	0	5.15	1.838520075	0	5.445	1.867068728	0	5.74	1.891928043	0
4.86	1.806590501	0	5.155	1.839036213	0	5.45	1.867520025	0	5.745	1.892319199	0
4.865	1.807174961	0	5.16	1.839551213	0	5.455	1.867970263	0	5.75	1.892709375	0
4.87	1.807758205	0	5.165	1.840065076	0	5.46	1.868419445	0	5.755	1.893098574	0
4.875	1.808340234	0	5.17	1.840577803	0	5.465	1.86886757	0	5.76	1.893486797	0
4.88	1.80892105	0	5.175	1.841089397	0	5.47	1.869314641	0	5.765	1.893874045	0
4.885	1.809500652	0	5.18	1.841599858	0	5.475	1.869760659	0	5.77	1.894260319	0
4.89	1.810079044	0	5.185	1.842109187	0	5.48	1.870205626	0	5.775	1.894645622	0
4.895	1.810656226	0	5.19	1.842617386	0	5.485	1.870649541	0	5.78	1.895029954	0
4.9	1.8112322	0	5.195	1.843124457	0	5.49	1.871092408	0	5.785	1.895413316	0
4.905	1.811806967	0	5.2	1.8436304	0	5.495	1.871534227	0	5.79	1.89579571	0
4.91	1.812380528	0	5.205	1.844135217	0	5.5	1.871975	0	5.795	1.896177138	0
4.915	1.812952885	0	5.21	1.84463891	0	5.505	1.872414728	0	5.8	1.8965576	0
4.92	1.813524038	0	5.215	1.845141479	0	5.51	1.872853412	0	5.805	1.896937098	0
4.925	1.814093991	0	5.22	1.845642926	0	5.515	1.873291054	0	5.81	1.897315634	0
4.93	1.814662743	0	5.225	1.846143253	0	5.52	1.873727654	0	5.815	1.897693208	0
4.935	1.815230296	0	5.23	1.846642461	0	5.525	1.874163216	0	5.82	1.898069822	0
4.94	1.815796651	0	5.235	1.84714055	0	5.53	1.874597739	0	5.825	1.898445478	0
4.945	1.816361811	0	5.24	1.847637523	0	5.535	1.875031225	0	5.83	1.898820177	0
4.95	1.816925775	0	5.245	1.848133381	0	5.54	1.875463675	0	5.835	1.899193919	0
4.955	1.817488546	0	5.25	1.848628125	0	5.545	1.875895092	0	5.84	1.899566707	0
4.96	1.818050125	0	5.255	1.849121756	0	5.55	1.876325475	0	5.845	1.899938542	0
4.965	1.818610513	0	5.26	1.849614277	0	5.555	1.876754827	0	5.85	1.900309425	0
4.97	1.819169711	0	5.265	1.850105687	0	5.56	1.877183149	0	5.855	1.900679357	0
4.975	1.819727722	0	5.27	1.850595989	0	5.565	1.877610442	0	5.86	1.901048341	0
4.98	1.820284546	0	5.275	1.851085184	0	5.57	1.878036707	0	5.865	1.901416376	0
4.985	1.820840184	0	5.28	1.851573274	0	5.575	1.878461947	0	5.87	1.901783465	0
4.99	1.821394638	0	5.285	1.852060258	0	5.58	1.878886162	0	5.875	1.902149609	0
4.995	1.82194791	0	5.29	1.85254614	0	5.585	1.879309353	0	5.88	1.90251481	0
5	1.8225	0	5.295	1.85303092	0	5.59	1.879731522	0	5.885	1.902879067	0

5.89	1.903242384	0
5.895	1.903604761	0
5.9	1.9039662	0
5.905	1.904326702	0
5.91	1.904686268	0
5.915	1.9050449	0
5.92	1.905402598	0
5.925	1.905759366	0
5.93	1.906115203	0
5.935	1.906470111	0
5.94	1.906824091	0
5.945	1.907177146	0
5.95	1.907529275	0
5.955	1.907880481	0
5.96	1.908230765	0
5.965	1.908580128	0
5.97	1.908928571	0
5.975	1.909276097	0
5.98	1.909622706	0
5.985	1.909968399	0
5.99	1.910313178	0
5.995	1.910657045	0
6	1.911	0
6.005	1.911342045	0
6.01	1.911683182	0
6.015	1.912023411	0
6.02	1.912362734	0
6.025	1.912701153	0
6.03	1.913038669	0
6.035	1.913375282	0
6.04	1.913710995	0
6.045	1.914045809	0
6.05	1.914379725	0
6.055	1.914712744	0
6.06	1.915044869	0
6.065	1.915376099	0
6.07	1.915706437	0
6.075	1.916035884	0
6.08	1.916364442	0
6.085	1.91669211	0
6.09	1.917018892	0
6.095	1.917344788	0
6.1	1.9176698	0
6.105	1.917993929	0
6.11	1.918317176	0
6.115	1.918639543	0
6.12	1.91896103	0
6.125	1.919281641	0
6.13	1.919601375	0
6.135	1.919920234	0
6.14	1.920238219	0
6.145	1.920555333	0
6.15	1.920871575	0
6.155	1.921186948	0
6.16	1.921501453	0
6.165	1.921815091	0
6.17	1.922127863	0
6.175	1.922439772	0
6.18	1.922750818	0
6.185	1.923061002	0
6.19	1.923370326	0
6.195	1.923678792	0
6.2	1.9239864	0
6.205	1.924293152	0
6.21	1.92459905	0
6.215	1.924904094	0
6.22	1.925208286	0
6.225	1.925511628	0
6.23	1.925814121	0
6.235	1.926115765	0
6.24	1.926416563	0
6.245	1.926716516	0
6.25	1.927015625	0
6.255	1.927313891	0
6.26	1.927611317	0
6.265	1.927907902	0
6.27	1.928203649	0
6.275	1.928498559	0
6.28	1.928792634	0
6.285	1.929085873	0
6.29	1.92937828	0
6.295	1.929669855	0
6.3	1.9299606	0
6.305	1.930250516	0
6.31	1.930539604	0
6.315	1.930827866	0
6.32	1.931115302	0
6.325	1.931401916	0
6.33	1.931687707	0
6.335	1.931972677	0
6.34	1.932256827	0
6.345	1.93254016	0
6.35	1.932822675	0
6.355	1.933104375	0
6.36	1.933385261	0
6.365	1.933665334	0
6.37	1.933944595	0
6.375	1.934223047	0
6.38	1.93450069	0
6.385	1.934777525	0
6.39	1.935053554	0
6.395	1.935328779	0
6.4	1.9356032	0
6.405	1.935876819	0
6.41	1.936149638	0
6.415	1.936421657	0
6.42	1.936692878	0
6.425	1.936963303	0
6.43	1.937232933	0
6.435	1.937501768	0
6.44	1.937769811	0
6.445	1.938037063	0
6.45	1.938303525	0
6.455	1.938569198	0
6.46	1.938834085	0
6.465	1.939098185	0
6.47	1.939361501	0
6.475	1.939624034	0
6.48	1.939885786	0
6.485	1.940146756	0
6.49	1.940406948	0
6.495	1.940666362	0
6.5	1.940925	0
6.505	1.941182863	0
6.51	1.941439952	0
6.515	1.941696269	0
6.52	1.941951814	0
6.525	1.942206591	0
6.53	1.942460599	0
6.535	1.94271384	0
6.54	1.942966315	0
6.545	1.943218027	0
6.55	1.943468975	0
6.555	1.943719162	0
6.56	1.943968589	0
6.565	1.944217257	0
6.57	1.944465167	0
6.575	1.944712322	0
6.58	1.944958722	0
6.585	1.945204368	0
6.59	1.945449262	0
6.595	1.945693406	0
6.6	1.9459368	0
6.605	1.946179446	0
6.61	1.946421346	0
6.615	1.9466625	0
6.62	1.94690291	0
6.625	1.947142578	0
6.63	1.947381505	0
6.635	1.947619691	0
6.64	1.947857139	0
6.645	1.94809385	0
6.65	1.948329825	0
6.655	1.948565065	0
6.66	1.948799573	0
6.665	1.949033348	0
6.67	1.949266393	0
6.675	1.949498709	0
6.68	1.949730298	0
6.685	1.949961159	0
6.69	1.950191296	0
6.695	1.950420709	0
6.7	1.9506494	0
6.705	1.95087737	0
6.71	1.95110462	0
6.715	1.951331152	0
6.72	1.951556966	0
6.725	1.951782066	0
6.73	1.952006451	0
6.735	1.952230123	0
6.74	1.952453083	0
6.745	1.952675334	0
6.75	1.952896875	0
6.755	1.953117709	0
6.76	1.953337837	0
6.765	1.95355726	0
6.77	1.953775979	0
6.775	1.953993997	0
6.78	1.954211314	0
6.785	1.954427931	0
6.79	1.95464385	0
6.795	1.954859073	0
6.8	1.9550736	0
6.805	1.955287433	0
6.81	1.955500574	0
6.815	1.955713023	0
6.82	1.955924782	0
6.825	1.956135853	0
6.83	1.956346237	0
6.835	1.956555934	0
6.84	1.956764947	0
6.845	1.956973277	0
6.85	1.957180925	0
6.855	1.957387892	0
6.86	1.957594181	0
6.865	1.957799791	0
6.87	1.958004725	0
6.875	1.958208984	0
6.88	1.95841257	0
6.885	1.958615482	0
6.89	1.958817724	0
6.895	1.959019296	0
6.9	1.9592202	0
6.905	1.959420437	0
6.91	1.959620008	0
6.915	1.959818915	0
6.92	1.960017158	0
6.925	1.960214741	0
6.93	1.960411663	0
6.935	1.960607926	0
6.94	1.960803531	0
6.945	1.960998481	0
6.95	1.961192775	0
6.955	1.961386416	0
6.96	1.961579405	0
6.965	1.961771743	0
6.97	1.961963431	0
6.975	1.962154472	0
6.98	1.962344866	0
6.985	1.962534614	0
6.99	1.962723718	0
6.995	1.96291218	0
7	1.9631	0
7.005	1.96328718	0
7.01	1.963473722	0
7.015	1.963659626	0
7.02	1.963844894	0
7.025	1.964029528	0
7.03	1.964213529	0
7.035	1.964396897	0
7.04	1.964579635	0
7.045	1.964761744	0
7.05	1.964943225	0
7.055	1.965124079	0
7.06	1.965304309	0
7.065	1.965483914	0

7.07	1.965662897	0
7.075	1.965841259	0
7.08	1.966019002	0
7.085	1.966196125	0
7.09	1.966372632	0
7.095	1.966548523	0
7.1	1.9667238	0
7.105	1.966898464	0
7.11	1.967072516	0
7.115	1.967245958	0
7.12	1.96741879	0
7.125	1.967591016	0
7.13	1.967762635	0
7.135	1.967933649	0
7.14	1.968104059	0
7.145	1.968273868	0
7.15	1.968443075	0
7.155	1.968611683	0
7.16	1.968779693	0
7.165	1.968947106	0
7.17	1.969113923	0
7.175	1.969280147	0
7.18	1.969445778	0
7.185	1.969610817	0
7.19	1.969775266	0
7.195	1.969939127	0
7.2	1.9701024	0
7.205	1.970265087	0
7.21	1.97042719	0
7.215	1.970588709	0
7.22	1.970749646	0
7.225	1.970910003	0
7.23	1.971069781	0
7.235	1.97122898	0
7.24	1.971387603	0
7.245	1.971545651	0
7.25	1.971703125	0
7.255	1.971860026	0
7.26	1.972016357	0
7.265	1.972172117	0
7.27	1.972327309	0
7.275	1.972481934	0
7.28	1.972635994	0
7.285	1.972789488	0
7.29	1.97294242	0
7.295	1.97309479	0
7.3	1.9732466	0
7.305	1.973397851	0
7.31	1.973548544	0
7.315	1.973698681	0
7.32	1.973848262	0
7.325	1.973997291	0
7.33	1.974145767	0
7.335	1.974293692	0
7.34	1.974441067	0
7.345	1.974587895	0
7.35	1.974734175	0
7.355	1.97487991	0
7.36	1.975025101	0
7.365	1.975169749	0
7.37	1.975313855	0
7.375	1.975457422	0
7.38	1.97560045	0
7.385	1.97574294	0
7.39	1.97584894	0
7.395	1.976026314	0
7.4	1.9761672	0
7.405	1.976307554	0
7.41	1.976447378	0
7.415	1.976586672	0
7.42	1.976725438	0
7.425	1.976863678	0
7.43	1.977001393	0
7.435	1.977138583	0
7.44	1.977275251	0
7.445	1.977411398	0
7.45	1.977547025	0
7.455	1.977682133	0
7.46	1.977816725	0
7.465	1.9779508	0
7.47	1.978084361	0
7.475	1.978217409	0
7.48	1.978349946	0
7.485	1.978481971	0
7.49	1.978613488	0
7.495	1.978744497	0
7.5	1.978875	0
7.505	1.979004998	0
7.51	1.979134492	0
7.515	1.979263484	0
7.52	1.979391974	0
7.525	1.979519966	0
7.53	1.979647459	0
7.535	1.979774455	0
7.54	1.979900955	0
7.545	1.980026962	0
7.55	1.980152475	0
7.555	1.980277497	0
7.56	1.980402029	0
7.565	1.980526072	0
7.57	1.980649627	0
7.575	1.980772697	0
7.58	1.980895282	0
7.585	1.981017383	0
7.59	1.981139002	0
7.595	1.981260141	0
7.6	1.9813808	0
7.605	1.981500981	0
7.61	1.981620686	0
7.615	1.981739915	0
7.62	1.98185867	0
7.625	1.981976953	0
7.63	1.982094765	0
7.635	1.982212106	0
7.64	1.982328979	0
7.645	1.982445385	0
7.65	1.982561325	0
7.655	1.9826768	0
7.66	1.982791813	0
7.665	1.982906363	0
7.67	1.983020453	0
7.675	1.983134084	0
7.68	1.983247258	0
7.685	1.983359974	0
7.69	1.983472236	0
7.695	1.983584044	0
7.7	1.9836954	0
7.705	1.983806305	0
7.71	1.98391676	0
7.715	1.984026767	0
7.72	1.984136326	0
7.725	1.984245441	0
7.73	1.984354111	0
7.735	1.984462338	0
7.74	1.984570123	0
7.745	1.984677469	0
7.75	1.984784375	0
7.755	1.984890844	0
7.76	1.984996877	0
7.765	1.985102475	0
7.77	1.985207639	0
7.775	1.985312372	0
7.78	1.985416674	0
7.785	1.985520546	0
7.79	1.98562399	0
7.795	1.985727008	0
7.8	1.9858296	0
7.805	1.985931768	0
7.81	1.986033514	0
7.815	1.986134838	0
7.82	1.986235742	0
7.825	1.986336228	0
7.83	1.986436297	0
7.835	1.986535949	0
7.84	1.986635187	0
7.845	1.986734012	0
7.85	1.986832425	0
7.855	1.986930427	0
7.86	1.987028021	0
7.865	1.987125206	0
7.87	1.987221985	0
7.875	1.987318359	0
7.88	1.98741433	0
7.885	1.987509897	0
7.89	1.987605064	0
7.895	1.987699831	0
7.9	1.9877942	0
7.905	1.98788172	0
7.91	1.987981748	0
7.915	1.98807493	0
7.92	1.988167718	0
7.925	1.988260116	0
7.93	1.988352123	0
7.935	1.988443741	0
7.94	1.988534971	0
7.945	1.988625816	0
7.95	1.988716275	0
7.955	1.988806351	0
7.96	1.988896045	0
7.965	1.988985358	0
7.97	1.989074291	0
7.975	1.989162847	0
7.98	1.989251026	0
7.985	1.989338829	0
7.99	1.989426258	0
7.995	1.989513315	0
8	1.9896	0
8.005	1.989686315	0
8.01	1.989772262	0
8.015	1.989857841	0
8.02	1.989943054	0
8.025	1.990027903	0
8.03	1.990112389	0
8.035	1.990196512	0
8.04	1.990280275	0
8.045	1.990363679	0
8.05	1.990446725	0
8.055	1.990529414	0
8.06	1.990611749	0
8.065	1.990693729	0
8.07	1.990775357	0
8.075	1.990856634	0
8.08	1.990937562	0
8.085	1.99101814	0
8.09	1.991098372	0
8.095	1.991178258	0
8.1	1.9912578	0
8.105	1.991336999	0
8.11	1.991415856	0
8.115	1.991494373	0
8.12	1.99157255	0
8.125	1.991650391	0
8.13	1.991727895	0
8.135	1.991805064	0
8.14	1.991881899	0
8.145	1.991958403	0
8.15	1.992034575	0
8.155	1.992110418	0
8.16	1.992185933	0
8.165	1.992261121	0
8.17	1.992335983	0
8.175	1.992410522	0
8.18	1.992484738	0
8.185	1.992558632	0
8.19	1.992632206	0
8.195	1.992705462	0
8.2	1.9927784	0
8.205	1.992851022	0
8.21	1.99292333	0
8.215	1.992995324	0
8.22	1.993067006	0
8.225	1.993138378	0
8.23	1.993209441	0
8.235	1.993280195	0
8.24	1.993350643	0
8.245	1.993420786	0

8.25	1.993490625	0
8.255	1.993560161	0
8.26	1.993629397	0
8.265	1.993698332	0
8.27	1.993766969	0
8.275	1.993835309	0
8.28	1.993903354	0
8.285	1.993971103	0
8.29	1.99403856	0
8.295	1.994105725	0
8.3	1.9941726	0
8.305	1.994239186	0
8.31	1.994305484	0
8.315	1.994371496	0
8.32	1.994437222	0
8.325	1.994502666	0
8.33	1.994567827	0
8.335	1.994632707	0
8.34	1.994697307	0
8.345	1.99476163	0
8.35	1.994825675	0
8.355	1.994889445	0
8.36	1.994952941	0
8.365	1.995016164	0
8.37	1.995079115	0
8.375	1.995141797	0
8.38	1.99520421	0
8.385	1.995266355	0
8.39	1.995328234	0
8.395	1.995389849	0
8.4	1.9954512	0
8.405	1.995512289	0
8.41	1.995573118	0
8.415	1.995633687	0
8.42	1.995693998	0
8.425	1.995754053	0
8.43	1.995813853	0
8.435	1.995873398	0
8.44	1.995932691	0
8.445	1.995991733	0
8.45	1.996050525	0
8.455	1.996109068	0
8.46	1.996167365	0
8.465	1.996225415	0
8.47	1.996283221	0
8.475	1.996340784	0
8.48	1.996398106	0
8.485	1.996455186	0
8.49	1.996512028	0
8.495	1.996568632	0
8.5	1.996625	0
8.505	1.996681133	0
8.51	1.996737032	0
8.515	1.996792699	0
8.52	1.996848134	0
8.525	1.996903341	0
8.53	1.996958319	0
8.535	1.99701307	0
8.54	1.997067595	0
8.545	1.997121897	0
8.55	1.997175975	0
8.555	1.997229832	0
8.56	1.997283469	0
8.565	1.997336887	0
8.57	1.997390087	0
8.575	1.997443072	0
8.58	1.997495842	0
8.585	1.997548398	0
8.59	1.997600742	0
8.595	1.997652876	0
8.6	1.9977048	0
8.605	1.997756516	0
8.61	1.997808026	0
8.615	1.99785933	0
8.62	1.99791043	0
8.625	1.997961328	0
8.63	1.998012025	0
8.635	1.998062521	0
8.64	1.998112819	0
8.645	1.99816292	0
8.65	1.998212825	0
8.655	1.998262535	0
8.66	1.998312053	0
8.665	1.998361378	0
8.67	1.998410513	0
8.675	1.998459459	0
8.68	1.998508218	0
8.685	1.998556789	0
8.69	1.998605176	0
8.695	1.998653379	0
8.7	1.9987014	0
8.705	1.99874924	0
8.71	1.9987969	0
8.715	1.998844382	0
8.72	1.998891686	0
8.725	1.998938816	0
8.73	1.998985771	0
8.735	1.999032553	0
8.74	1.999079163	0
8.745	1.999125604	0
8.75	1.999171875	0
8.755	1.999217979	0
8.76	1.999263917	0
8.765	1.99930969	0
8.77	1.999355299	0
8.775	1.999400747	0
8.78	1.999446034	0
8.785	1.999491161	0
8.79	1.99953613	0
8.795	1.999580943	0
8.8	1.9996256	0
8.805	1.999670103	0
8.81	1.999714454	0
8.815	1.999758653	0
8.82	1.999802702	0
8.825	1.999846603	0
8.83	1.999890357	0
8.835	1.999933964	0

Appendix E: SST Variable Definitions and Constants

$$P = \tau_7 \frac{\delta u_7}{\delta x}$$

$$\tau_7 = \mu - 2S_7 - \frac{2}{3} \frac{\delta u}{\delta x} - \delta_7 - \frac{2}{3} \rho k \delta_7$$

$$S_7 = \frac{1}{2} \frac{\delta u_7}{\delta x} + \frac{\delta u_7}{\delta x_7}$$

$$\mu = \frac{\rho a k}{\max(a \omega, \Omega F)}$$

$$\phi = F \phi + (1 - F) \phi$$

$$F = \tanh(\arg)$$

$$\arg = \max 12 \frac{\sqrt{k}_*}{\beta \varpi d} \frac{500 \nu_7}{d \omega}$$

$$\sigma = 0.85$$

$$\sigma = 0.65$$

$$\beta = 0.075$$

$$\sigma = 1.00$$

$$\sigma = 0.856$$

$$\beta = 0.0828$$

$$\beta^* = 0.09$$

$$\alpha = 0.31$$